Title: Microbial eukaryotic distributions and diversity patterns in a deep-sea methane seep ecosystem

Authors: Alexis L. Pasulka[1,2*], Lisa A. Levin[1], Josh A. Steele[2,3], David H. Case[2], Michael R. Landry[1], Victoria J. Orphan[2]

[1]Integrative Oceanography Division and Center for Marine Biodiversity and Conservation, Scripps Institution of Oceanography, University of California, San Diego, La Jolla, CA, USA

[2]Division of Geological and Planetary Sciences, California Institute of Technology, Pasadena, CA, USA

[3]Now at Southern California Coastal Water Research Project, Costa Mesa, CA, USA

Running Title: Microbial eukaryotic patterns in deep-sea methane seeps

Keywords: Microbial eukaryote, methane seep, microbial ecology

***Corresponding Author:** apasulka@caltech.edu

This article has been accepted for publication and undergone full peer review but has not been through the copyediting, typesetting, pagination and proofreading process, which may lead to differences between this version and the Version of Record. Please cite this article as doi: 10.1111/1462-2920.13185

Summary

Although chemosynthetic ecosystems are known to support diverse assemblages of microorganisms, the ecological and environmental factors that structure microbial eukaryotes (heterotrophic protists and fungi) are poorly characterized. In this study, we examined the geographic, geochemical and ecological factors that influence microbial eukaryotic composition and distribution patterns within Hydrate Ridge, a methane seep ecosystem off the coast of Oregon using a combination of high-throughput 18S rRNA tag sequencing (iTAG), terminal restriction fragment length polymorphism fingerprinting (T-RFLP) and cloning and sequencing of full-length 18S rRNA genes. Microbial eukaryotic composition and diversity varied as a function of substrate (carbonate vs. sediment), activity (low activity vs. active seep sites), sulfide concentration, and region (North vs. South Hydrate Ridge). Sulfide concentration was correlated with changes in microbial eukaryotic composition and richness. This work also revealed the influence of oxygen content in the overlying water column and water depth on microbial eukaryotic composition and diversity and identified distinct patterns from those previously observed for bacteria, archaea and macrofauna in methane seep ecosystems. Characterizing the structure of microbial eukaryotic communities in response to environmental variability is a key step towards understanding if and how microbial eukaryotes influence seep ecosystem structure and function.

Introduction

Methane seeps are common to most of the world's continental margins and play an important role in the global carbon cycle (German *et al.*, 2011). Subsurface frozen hydrates are earth's largest methane reservoir, estimated at 500–2500 Gt of carbon (Milkov 2004). Chemosynthetic microbes within seep sediments act as a biological filter, providing an important control mechanism on flux of methane from the sediments into the water column (Valentine *et al.*, 200l; Sommer *et al.*, 2006). Therefore, any process that influences community composition, abundance, or methane utilization rates of these chemosynthetic prokaryotes in seeps not only affects the efficiency of this biological filter, but also impacts overall ecosystem structure and function. While extensive research has characterized the bacterial, archaeal, and metazoan communities living at methane seeps (e.g., Levin, 2005; Orphan *et al.*, 2001; Knittel and Boetius, 2009; Cordes *et al.*, 2010; Valentine, 2011, Ruff *et al.*, 2015), studies on microbial eukaryotes are rare. In pelagic ecosystems, microbial eukaryotes are the primary consumers of phytoplankton, heterotrophic bacteria and archaea (Sherr and Sherr, 1994; 2000), utilizing more than two-thirds of ocean primary productivity (Calbet and Landry, 2004). In addition, they serve as important trophic links in transferring carbon between the microbial food web and the metazoan food web (Sherr and Sherr, 1988; 1994). However, the ecological roles of microbial eukaryotes are poorly understood for methane seep ecosystems.

Microbial eukaryotes have only started to be recognized as integral components of reducing habitats. Molecular surveys of suboxic and anoxic waters (Behnke *et al.*, 2006; Edgcomb *et al.*, 2011c; Wylezich and Jurgens, 2011), hydrothermal vents (Edgcomb *et al*., 2002; López-García *et al.*, 2007; Coyne et al 2013), and methane seeps (Takishita *et al.*, 2007; 2010) have revealed a great diversity of microbial eukaryotes and in some instances evidence of novel

lineages and endemism. Preliminary evidence also suggests that microbial eukaryotes are involved in food web interactions within reducing ecosystems (Murase *et al.*, 2006; Murase and Frenzel, 2008; Anderson et al. 2012; 2013). Additionally, symbiotic interactions (Edgcomb *et al.*, 2011a, b) and grazing (Sherr and Sherr, 1994; 2002) are likely to have significant impacts on bacterial and archaeal community structure and carbon and nitrogen cycling, but remain largely unexplored in deep-sea chemosynthetic ecosystems.

Identifying the ecological and environmental factors that structure microbial eukaryotic communities in methane seeps is therefore important for characterizing ecosystem function as well as the ecology of these unique habitats. Environmental heterogeneity in seeps can be found at scales ranging from centimeters to kilometers due to variability in fluid flow, geochemistry, and associated fauna and seep location along continental margins (Cordes *et al*., 2009). Within seep sediments, the rates and magnitude of methane flux, as well as the distributions and activities of methane-consuming archaea and sulfate-reducing bacteria, vary vertically and with distance away from active seep sites (Sahling *et al.*, 2002, Treude *et al.*, 2003, Levin *et al.*, 2003). Such variability greatly influences pore water geochemistry and creates heterogeneity at the smallest scales (micrometers to tens of centimeters) (Treude *et al.*, 2003; Orphan *et al.*, 2004; Gieskes *et al.*, 2005). Distinct biogenic habitats (e.g., clam beds, microbial mats and carbonate rocks) form within meters of one another in response to this small-scale variability in geochemistry and microbial activity and create an additional scale of heterogeneity within seep ecosystems (Levin 2005; Cordes *et al.*, 2009).

Certain seeps, such as Hydrate Ridge (HR) along the Cascadia Margin, are situated where permanently low oxygen conditions overlay the seafloor. Here the oxygen minimum zone (OMZ) extends from approximately 650 to 1100 m water depth, reaching the lowest oxygen

levels around 800 m (Helly and Levin, 2004). Therefore, the southern extent of HR (800 m; called South HR) is located within the OMZ with oxygen concentrations typically less than 0.5 ml l^{-1} with reports as low as 0.2 ml l^{-1}, while the northern extent of HR (North HR; 590 m) is located just outside the OMZ with oxygen concentrations ranging from 0.5-0.8 ml l^{-1} (Levin *et al.*, 2010). In this location, oxygen in waters overlying the seabed creates another scale of heterogeneity that may influence microbial eukaryotic community composition and diversity between seep regions (e.g., kilometer-scale variability).

The range of environmental conditions at HR has made it a 'natural laboratory' for extensive research that has explored the biology and geochemistry of seep systems (Boetius and Suess, 2004). It is thus an ideal site in which to integrate microbial eukaryotes into our understanding of seep ecology. Previous work at HR and other methane seeps has shown that the distributions, abundances, and diversities of meiofaunal and macrofaunal metazoans are influenced by all of the scales of heterogeneity described above (Montagna *et al.*, 1989; Dando *et al.*, 1991; Sahling *et al.*, 2002; Levin, 2005; Cordes *et al.*, 2009; Levin *et al.*, 2010; Guillini *et al.*, 2012).

Here we characterize the microbial eukaryotic community across these scales of environmental heterogeneity at HR (i.e., centimeter-scale within habitat variability, meter-scale between habitat variability and kilometer-scale regional variability) using a combination of molecular methods: massively-parallel high-throughput tag sequencing targeting the V9 hypervariable region of the 18S ribosomal RNA (rRNA) gene (iTAG), terminal restriction fragment length polymorphism (T-RFLP) fingerprinting, and cloning and sequencing of full-length 18S rRNA genes. The goal of this study is to go beyond the characterization of protistan diversity in seep environments and to examine the geographic, geochemical and ecological

factors that influence microbial eukaryotic composition and distribution patterns within seep habitats. We test the hypotheses that (1) microbial eukaryotic communities associated with active seeps are more similar to one another than those from sites with lower methane flux (i.e., low activity sites), (2) the composition and diversity of sediment-hosted microbial eukaryotes varies in relation to sulfide gradients, and (3) that these patterns may vary regionally as a result of differences in water depth and/or oxygen concentration of the overlying water between North and South HR.

Results

Environmental characteristics

Depth profiles for all push cores were analyzed for concentrations of sulfide (HS^-) and sulfate (SO_4^{2-}). HS^- and SO_4^{2-} profiles in the sediments underlying microbial mats were different than the profiles under clam beds (Fig. 2). In general, the pore water profiles were characteristic of their respective habitat types (Sahling *et al.*, 2002, Treude *et al.*, 2003, Orphan *et al.*, 2004, Gieskes *et al.*, 2005), with rapid SO_4^{2-} depletion at shallower depths in microbial mat cores relative to cores from the bioturbated clam beds. However, variability was observed within like-type habitats. For example, HS^- concentrations were 2 to 2.5 times greater in microbial mat cores from South HR (average 0-3 cm = 10.9 ± 5.6 mM, average 3-6 cm = 17.6 ± 1.6 mM, and average 6-9 cm 19.0 ± 2.8 mM) compared to North HR (average 0-3 cm = 4.3 ± 1.5 mM, average 3-6 cm = 7.1 ± 5.7 mM and average 6-9 cm = 7.6 ± 4.5 mM). HS^- concentrations within the clam cores, however, were not significantly different between North and South HR. The off-seep inactive cores had a distinct profile compared to the active seep cores, with pore water HS^- remaining below detectable limits while SO_4^{2-} was approximate 25 mM throughout the upper 9 cm (Fig. 2).

Community composition and diversity estimates based on 18S rRNA gene clone libraries

Our three clone libraries, one from each depth in a microbial mat core collected from North HR, were composed predominantly of protistan sequences (92%, 83% and 82% in the 0-3, 3-6 and 6-9 cm depth horizons, respectively). Metazoans comprised approximately 10% of the libraries across all depths, while fungi contributed a greater proportion with increasing sediment depth (1% at 0-3 cm, 7% at 3-6 cm and 12% at 6-9 cm). A total of 46, 24 and 20 protistan OTUs were identified in the clone libraries from 0-3, 3-6 and 6-9 cm sediment depths, respectively. Ciliates made up 90, 50 and 72% of the protistan taxa in the three libraries (0-3 cm, 3-6 cm and 6-cm, respectively), with lower proportions of other protistan groups (Fig. S2). Apicomplexa, Dinoflagellata, Stramenopiles, Cercozoa, Amoebozoa and Excavata (superphylum Discoba) were among the other protistan lineages recovered from our clone library sequences. Cercozoa and Apicomplexa comprised a greater proportion of the protistan community in the 3-6 cm clone library (20 and 15%, respectively) than the 0-3 cm library (2 and 1.2%, respectively), and were entirely absent from the 6-9 cm library. Amoebozoa made up approximately 10% of the protistan community in the 3-6 and 6-9 cm depth horizons, but were absent at 0-3 cm depth.

Given the large percentage of ciliate sequences in our clone libraries, we chose to focus predominantly on this group. Sequences were identified from six previously recognized ciliate classes (Adl *et al.* 2005) as well as a novel clade of deep-sea ciliates (Takishita *et al.*, 2010) and the recently described class Cariacotrichea (Orsi *et al.*, 2012a) (Fig. 3). Ciliates from the Spirotrichea were found only in the in 0-3 cm sediment horizon (Fig. 4A). The novel clade of deep-sea ciliates comprised a significant portion of the community in the 0-3 cm (53 %) and 3-6 cm (38 %) sediment horizons, but only comprised 10% of the community in the 6-9 cm horizon

(Fig. 4A). Ciliates from Plagiopylea were found only in the upper six centimeters of the sediment, whereas Cariacotrichea increased in relative abundance with increasing sediment depth (Fig. 4A). Ciliates from Litostomatea, Armophorea and Oligohymenophorea were most abundant at 6-9 cm depth.

Community composition patterns based on high-throughput 18S rRNA gene sequencing

High-throughput sequencing identified a total of 3,492,014 reads of which 3,048,275 were high quality (Table S1). Contribution from metazoan sequences varied greatly across the samples, ranging from 1%-90% of the sequence total and decreasing generally with increasing sediment depth. Fungal sequences made up a small fraction (0.001% to 0.2%) of the iTAG libraries. After filtering out non-target sequences (e.g., bacteria, archaea, and metazoans), we identified 189,126 quality V9 sequences for microbial eukaryotes (including fungi).

Microbial eukaryotic communities were differentiated by substrate type (Fig. 5 and Table 1; ANOSIM $p = 0.001$, global $R = 0.4$) and seep activity (ANOSIM $p = 0.001$, global $R = 0.3$) when all sediment and carbonate samples were considered together. Carbonates were only examined in the iTAG data set and were differentiated by activity (Table 1; ANOSIM $p = 0.04$, $R = 0.3$). Further examination of just the sediment habitats (microbial mats, clam beds and low activity sediments) indicated significant effects of region (ANOSIM $p = 0.01$, global $R = 0.2$) in addition to activity (ANOSIM $p = 0.001$, global $R = 0.5$) and habitat type (ANOSIM $p = 0.001$, global $R = 0.2$) on microbial eukaryotic composition (Fig. 6A and Table 1). Pairwise comparisons between habitat types showed that while microbial mat and clam bed cores had significantly different communities from low activity sediments ($p_{mat, ref} = 0.001$, $p_{clam, ref} = 0.004$), the microbial mat and clam bed microbial eukaryotic communities were not significantly

different from one another ($p_{mat, clam} = 0.4$). Microbial eukaryotic communities were differentiated by depth when considering all sediment habitats collectively (ANOSIMS p = 0.01, global R = 0.2). Microbial eukaryotic communities were differentiated by sulfide concentration (Fig. 6A) when considering all sediments (ANOSIM p = 0.001, global R = 0.4), active sediments (ANOSIM p = 0.009, global R = 0.3) and microbial mat sediments (ANOSIM p = 0.001, global R = 0.5). While sulfide was not observed to be a significant factor for microbial eukaryotes in clam bed sediments, pairwise comparisons did reveal that microbial eukaryotic communities living at low sulfide concentrations (less than 3 mM) were significantly different from those communities living at high sulfide concentrations (greater that 9 mM) (p-values ranging from 0.03-0.05). While the data shown in Figs. 5 and 6 and the ANOSIM results in Table 1 are derived from the iTAG-L4 data set (for best comparison with T-RFLP data), the patterns were consistent in the iTAG-OTU data set as well (Table S3, Fig. S3).

The relative abundances of microbial eukaryotic classes varied across all the samples (Fig. 7, Fig. S4). OTU richness within each class also varied, but most taxonomic classes had 1-3 OTUs (Fig. S5). Groups with the highest relative abundances (and OTU richness) in the iTAG library included Bacilliarophyta, Dinophyta, Filosa-Thecofilosa, Polycystina and Apicomplexa (Fig. S4). Most members of these groups either contain some sort of shell (test or theca) and/or are known to be spore formers. We address the implications of this in terms of DNA surveys (*e.g.*, PCR and sequencing biases, copy number of ribosomal genes) in the discussion and supplemental material. We identified the microbial eukaryotic groups that contributed the most to differences in composition between substrate type and activity using SIMPER (Fig. 7). Fungi (Basidomycota and Ascomycota) and Foraminifera (Rotaliida and monothalamids) contributed to the differences in composition between carbonates and sediments, with all groups having

higher relative abundances on carbonates (SIMPER and Fig. 7). OTU richness within the observed fungal and foraminiferal groups was also higher on carbonates compared to sediments (Fig. S5). Foraminifera (Rotaliida and monothalamids) also contributed to differences between active and low activity sediments, having greater relative abundances (and higher OTU richness) in low activity sediments (SIMPER, Fig. 7, Fig. S5). The relative abundance of protists within the Phylums Cercozoa and Amoebozoa varied between substrates. Cercozoa within the Novel Clade-12 had higher relative abundances in sediments compared to carbonates, regardless of activity. However, Cercozoa within the Chlorarachnea had higher abundances on carbonates compared to sediments (SIMPER and Fig. 7). Although having low overall abundances, Amoebozoa (both Breviatea and Lobosa) had higher relative abundances in sediments compared to carbonates, regardless of activity. Within the sediments, however, Breviatea had higher relative abundances in active sediments, whereas Lobosa had higher relative abundances in inactive sediments (SIMPER and Fig. 7).

Ciliates also contributed to the variability between sample groups. Ciliates within the classes Armophorea and Cariacotrichea had higher abundance in active sediments relative to active carbonates (SIMPER and Fig. 7). Within sediment habitats, most ciliate classes (with the exception of Heterotrichea, Prostomatea, and Plagiopylea) had higher relative abundances in active sediments compared to inactive sediments. Similarly, ciliates had higher relative abundances on active carbonates (with the exception of Prostomatea and Heterotrichea) compared to inactive carbonates. Within the ciliate classes, Oligohymenophorea, Spirotrichea, and Litostomatea had the greatest OTU richness across all samples (Fig. S5).

SIMPER analysis also revealed that ciliates contributed the most to differences in microbial eukaryotic composition at different sulfide concentrations. Therefore, we analyzed the

222 relative abundance of different ciliate groups in relationship to sulfide concentration (Fig. 4B).
223 Some ciliate classes, including Plagiopylea and Prostomatea, exhibited highest abundances at
224 low sulfide levels and decreased in relative abundances with increasing sulfide concentrations.
225 Other classes, including the Armophorea, Cariacotrichea and Litostomatea, exhibited a different
226 pattern, with highest abundances at mid-sulfide levels (9-12 mM). Oligohymenophorea had a
227 similar pattern, but had highest abundances around 12-15 mM of sulfide. It is important to note
228 that iTAG sequences that fell into the novel seep clade (as determined by placing this subset of
229 short reads onto the tree), as well as the sequences belonging this clade recovered by Takishita et
230 al. (2010) were assigned to the class Colpodea in the PR2 database. Colpodea relative abundance
231 exhibited two peaks – one at low sulfide levels and another around 12-15 mM of sulfide.
232
233 *Community composition patterns of microbial eukaryotes based on T-RFLP*
234 The relationships between microbial eukaryotic community composition and
235 environmental variables in the T-RFLP data were almost identical to the patterns observed with
236 the iTAG-L4 data set (Fig. 6; Table 1). When comparing microbial eukaryotic communities
237 across all sediments, we observed significant effects were found for region, activity and habitat
238 type (Fig. 6). As in the iTAG-L4 data set, microbial eukaryotic composition was also influenced
239 by sediment depth and sulfide concentration when considering all sediments (Fig. 6, Table 1).
240
241 *Diversity patterns of microbial eukaryotes*
242 Richness (S) and Shannon Diversity (H') varied within and across each habitat type
243 (Tables 2 and 3) as well as regionally (North vs. South HR). While absolute richness numbers
244 were biased by the data set (i.e., T-RFLP, iTAG-L4 and iTAG-OTU), the patterns within each

data set likely reflect real changes in diversity in response to environmental variability. On average, we observed higher microbial eukaryotic diversity (richness and H') in South HR across all habitats and all sample sets (with the exception of clam beds and carbonates from the iTAG-OTU data set; Tables 2 and 3). We also observed generally higher diversity in low activity sediments, relative to active sediments (Table 2), as well as higher diversity on low activity relative to active carbonates (Table 3). At the class level, there was no difference in the richness of microbial eukaryotes on active carbonates relative to active sediments. However, active carbonates had lower OTU richness than active sediments, particularly at South HR. Richness in the sediments was negatively correlated with sulfide concentration (Fig. 8), but the relationship was strongest when the data were separated by region (e.g., HR North and HR South).

Discussion

In this study, we combined several molecular approaches to explore how microbial eukaryotic community composition and diversity vary in relationship to environmental factors within methane seep ecosystems. T-RFLP, a high throughput, but low resolution fingerprinting method, remains a cost effective way to examine a large number of samples (Dorst *et al.*, 2014). The 18S rRNA gene clone libraries, created from three depths in a representative microbial mat core, provided valuable contextual information for interpreting our T-RFLP data as well as full-length 18S sequences for further phylogenetic comparisons within the Phylum Ciliophora. Massively parallel high-throughput tag sequencing, although lower taxonomic resolution than full-length sequencing, enabled us to obtain more extensive data for the entire sample set, while still yielding some taxonomic information (conservatively class level). This type of sequencing approach has been successfully applied to explore microbial eukaryotes in other types of

environments (e.g., Amaral-Zettler *et al.*, 2009, 2014; Stoeck *et al.*, 2009; Edgcomb *et al.*, 2011c) and unlike the T-RFLP data, this type of data provided us the ability to explore the distribution patterns of different groups of microbial eukaryotes, particularly ciliates. Our results are consistent with other recent studies that show high-throughput sequencing approaches do, in fact, reveal the same broad patterns as fingerprinting approaches (Pilloni *et al.*, 2012; Dorst *et al.*, 2014). Therefore, while we observe some differences between methodologies (discussed below as relevant), we focus our discussion on understanding how and why different scales of habitat heterogeneity structure the microbial eukaryotic communities of methane seep ecosystems, rather than a comparison of molecular approaches. However, it is important to acknowledge that interpreting 18S rRNA surveys in terms of relative abundance and diversity estimates can be problematic because of different copy numbers of SSU rRNA genes between taxa (Medinger *et al.*, 2010; Gong *et al.*, 2015), extraction methods (Santos *et al.*, 2015), PCR biases (e.g., primer biases, preferential amplification of some taxa) (Medinger *et al.*, 2010; Stoeck *et al.*, 2010; 2014; Adl *et al.*, 2014), sequencing errors (Lee *et al.*, 2012; Kunin *et al.*, 2013), and amplification of remnant DNA (e.g., e-DNA; Lorenz and Wackernagel 1987, Pawlowski *et al.*, 2011) (see supplemental material for a more detailed discussion of these sequencing biases). Acknowledging these biases, and in order to minimize their influence on interpreting our data, we focus our discussion on specific taxa across environmental gradients. This tends to be a more conservative interpretation than directly comparing multiple taxa within a sample where SSU rRNA gene copy number as well as PCR and sequencing biases can more greatly influence the apparent trends (Trembath-Reichert *et al.*, unpublished). Additionally, our whole-community observations in iTAG are well-supported by complementary the TRFLP technique (Fig. 6).

We hypothesized that microbial eukaryotic communities associated with active seep sites are more similar to one another than those from sites with lower methane flux (i.e., low activity sites). We showed that microbial eukaryotic communities in active seep environments were distinct from those communities in adjacent low activity habitats (Figs. 5 and 6). This finding is consistent with the discovery of novel species and lineages from previous molecular surveys of active seep sediments (Takishita *et al.*, 2007; 2010) as well as from other reducing habitats (e.g., Stoeck *et al.*, 2003; López-García *et al.*, 2007; Behnke *et al.*, 2010; Edgcomb *et al.*, 2009; Orsi *et al.*, 2011). However, unlike we hypothesized, all active habitats did not have the same composition of microbial eukaryotes. Active seep sediments (microbial mats and clam beds) hosted a different community from active carbonates suggesting that substrate, not just activity, plays an important role in structuring microbial eukaryotic communities within seep environments (Fig. 5). This observation is consistent with the recent finding that bacterial assemblages at Hydrate Ridge are also strongly influence by substrate type (Marlow *et al*., 2014). Although interestingly, archaeal assemblages appear to be influenced more by activity than by substrate (Marlow *et al*., 2014). We did observe variations in the composition and diversity of sediment-hosted microbial eukaryotes in relationship to sulfide concentration. However, because steep geochemical gradients vary vertically within the sediments (Fig. 2), we also found a significant relationship between microbial eukaryotic composition and sediment depth. The lack of depth as a factor influencing community composition when inactive sediments and clam beds were considered separately supports the notion that strong biogeochemical gradients in active sediments (the strongest of which are often observed in microbial mats), not just sediment depth, influenced microbial eukaryotic distribution and composition. And finally, as we hypothesized, microbial eukaryotic composition and diversity patterns did vary regionally.

By integrating our observations across all of this spatial heterogeneity found at Hydrate Ridge, we can now begin to hypothesize about the combinations of ecological and environmental factors that are operating to structure microbial eukaryotic communities within seep ecosystems.

Environmental factors influencing microbial eukaryotic community structure and diversity patterns within methane seep ecosystems

Based on a synthesis of our observations, we hypothesize that geochemical tolerances as well as chemosynthetic production rates and/or prey availability play significant roles in structuring microbial eukaryotic composition at smaller spatial scales within methane seeps (centimeters to meters). However, the input of surface-derived particulate organic carbon and oxygen levels in the overlying water column also appear to play an important role in structuring microbial eukaryotic communities, and may be responsible for differences in microbial eukaryotic composition and richness between seeps in different regions (i.e., kilometer-scale variability).

The different biogenic habitats (e.g., clam beds, microbial mats and carbonates) that occur at Hydrate Ridge as a result of variations in fluid flux and microbial activity (Tryon and Brown, 2001; Sahling *et al.*, 2002; Levin *et al.*, 2003, 2010) have been shown to influence metazoan macrofaunal community composition (e.g., polychaetes, snails) (Sahling *et al.*, 2002; Levin *et al.*, 2010, Levin *et al.*, 2015). It has been hypothesized that macrofaunal communities benefit from the increased structural complexity as well as higher oxygen concentrations (and lower sulfide levels) associated with clam beds (Levin *et al.*, 2010). Interestingly, we were not able to distinguish between the microbial eukaryotic communities associated with clam beds and microbial mats, nor did we observe any significant difference in diversity (richness and Shannon

diversity) between these two habitats. A recent study by Guilini *et al.* (2012) also found that metazoan meiofaunal communities (particularly nematodes) associated with microbial mats and clam beds were not distinguishable from one another. Together, these studies suggest that metazoan meiofauna and microbial eukaryotes are not affected in the same way by these habitat features as metazoan macrofauna, perhaps reflecting their different sensitivities or requirements for oxygen and sulfide. However, we are not able to rule out the possible influences of structural complexity associated with clams on microbial eukaryotic community composition (or diversity), because we only sampled the sediments. Microbial eukaryotes attached to clam shells are likely different than those dwelling in the sediments and may add to the overall diversity of microbial eukaryotes in this habitat.

Notably, we did observe a difference in the composition of microbial eukaryotes associated with carbonates compared to sediments (e.g., foraminifera and fungi had higher abundances on carbonates). However, there was no difference in the richness of microbial eukaryotes at the class level on carbonates relative to sediments. On the other hand, active carbonates had lower OTU richness than active sediments, particularly at South HR. These microbial eukaryotic patterns differ for metazoan macrofauna as well as bacteria and archaea. At Costa Rican seep sites, macrofauna had considerably higher diversity on active carbonates relative to active sediments and low activity carbonates (Levin *et al.*, 2015). At Hydrate Ridge active carbonates have been observed to host active and unique bacterial and archaeal communities (Marlow *et al.*, 2014a, b) that are more diverse than sediment-hosted communities (Case *et al.*, 2015). While we were able to identify some differences in microbial eukaryotic communities living on carbonates, the use of hard substrates as habitat for microbial eukaryotes in seeps requires further investigation.

Variations in sulfide, methane and oxygen have all been shown to affect distributions and compositions of microbial eukaryotic communities in other types of reducing habitats (Orsi *et al.*, 2011, 2012b; Edgcomb *et al.*, 2011c; Wylezich and Jurgens, 2011; Behnke *et al.*, 2006). These patterns may be related to varying tolerances to high sulfide and/or low oxygen concentrations or the ability of some microbial eukaryotic species to form symbiotic associations (Edgcomb *et al.*, 2011a, b). However, at seeps pore water sulfide concentrations are not only correlated with numerous other chemical compounds (e.g., sulfate, methane), but also with a variety of microbial processes (e.g., sulfate-dependent anaerobic oxidation of methane, AOM; Boetius *et al.*, 2000; Orphan *et al.*, 2001; Treude *et al.*, 2003). Therefore, while sulfide concentration was correlated with shifts in microbial eukaryotic community composition and diversity, other factors such as the rates and distributions of chemosynthetic production may play a larger role than currently recognized in shaping microbial eukaryotic communities within these reducing environments.

Very little is known about the food sources for protists in deep-sea methane seeps. While some microbial eukaryotes may utilize symbionts for energy (Buck *et al.*, 2000; Edgcomb *et al.*, 2011a, b), many are likely to be microaerophilic or anaerobic phagotrophs (Fenchel and Finlay 1990a, 1995). Although some anaerobic ciliates are predatory and can feed on smaller flagellates and ciliates, most protists in these habitats are probably bacterivorous (Fenchel *et al.*, 1990). Theoretical models suggest that the ratio between predator and prey biomass is proportional to gross growth efficiency (GGE) of the predator (Kerr, 1974; Platt and Denman, 1977). Aerobic protists, at least in the pelagic realm, are thought to have gross growth efficiencies ranging from 30-40% (Straile, 1997). Gross growth efficiencies of anaerobic protists, on the other hand, are approximately one quarter (GGE ≈ 10%) of those for aerobes (Fenchel and Finlay, 1990a). This

suggests, and is supported by empirical data (summarized in Fenchel and Finlay, 1990a), that predator-prey biomass ratios in anaerobic environments must be significantly lower (~25 %) than those in aerobic environments. Therefore, food availability likely plays a critical role in structuring microbial eukaryotic communities in deep-sea methane seep ecosystems.

The relative abundance patterns of ciliates in relationship to sulfide concentration from our study can provide some insight into the importance of food availability to microbial eukaryotic communities. The vertical distributions of AOM, sulfate reduction (SR) and the microbial consortia mediating AOM have been well characterized at HR (e.g., Treude *et al.*, 2003). Subsurface production peaks for both SR and AOM coincide with the sulfate-methane transition zone (sulfate levels ~10-15 mM) and the abundance peak for microbial consortia is usually just above these production peaks. As sulfate and sulfide are often inversely related in seep sediments (this study; Sommer *et al.*, 2006, Orphan *et al*., 2004), these production peaks correspond to a sulfide level of ~10-12 mM. The observed relative abundance peaks of several groups of ciliates including the Oligohymenophorea, Armophorea, Litosomatea and Cariacotrichea within this sulfide range is consistent with the hypothesis that these organisms are responding to areas of high productivity and high concentrations of prey. The ecologies of some of the different ciliate groups are discussed in more detail in the section below. Direct measurements of grazing or predator-prey biomass ratios are lacking for protists at seeps, but there is some evidence to support the notion that protists actively graze on seep-associated prokaryotes in both aerobic and anaerobic sediments (Werne *et al.*, 2002).

While abundance distributions of microbial eukaryotes tend to follow biogeochemical gradients in seep sediments, similarities in depth-integrated sulfate reduction and methane oxidation rates (Treude et al., 2003) might explain why clam beds and microbial mats can

406 support similar overall microbial eukaryotic communities despite distinctly different sulfide and
407 oxygen profiles. Microaerophilic protists are known to tolerate prolonged exposure to anoxia and
408 are able to survive on fermentative metabolism (Fenchel and Finlay, 1995; Finlay *et al.*, 1986),
409 and many anaerobes have adaptive responses to cope with periodic exposure to oxygen (Fenchel
410 and Finlay, 1990b, Fenchel and Finlay, 1991). Therefore, protists able to tolerate steep, but
411 fluctuating redox gradients, may gain a competitive advantage over other protists by living in
412 areas of high food concentration and microbial activity.
413 The input of surface-derived production into seep habitats could be an additional factor
414 influencing protistan composition regionally and is thought to play an important role in diversity
415 patterns in the deep sea. Diversities of foraminifera and metazoan macrofauana have been
416 observed to increase with increasing depth and decreasing particulate organic carbon (POC) flux
417 (Gooday *et al.*, 2001; Levin *et al.*, 2001). Chemosynthetic habitats are generally thought to be the
418 exception to this rule as a result of *in situ* chemosynthetic production. Animal communities in
419 chemosynthetic habitats can exhibit lower diversity, but higher dominance (and densities)
420 relative to the surrounding deep sea (Dando *et al.*, 1994; Sahling *et al.*, 2002). However, water
421 depth can influence whether or not seep macrofauna form dense and distinct assemblages
422 relative to non-seep habitats (reviewed in Levin 2005). At deeper depths, inputs of
423 photosynthetically-derived carbon are reduced, creating a greater reliance of these communities
424 on chemosynthetic production (Levin and Michener, 2002, Levin and Mendoza, 2007).
425 Therefore, we might expect that low activity sediments would have higher diversity of microbial
426 eukaryotes than active sediments, with regional variability as a result of differences in water
427 depth between North and South HR. In South HR, microbial eukaryotic diversity was higher in
428 low activity sediments compared to active sediments for the upper 0-3 cm horizon (t-test p-value

= 0.04; Table 2), a pattern that is consistent with a recent survey of Guaymas Basin vent sediments (~2000 m; Coyne *et al.*, 2013). For North HR, on the other hand, we observed no significant difference in diversity between low activity and active sites. As North HR is shallower than both South HR and Guaymas Basin, this regional diversity difference is consistent with the food flux hypothesis, with additional surface-derived POC input to the seafloor in North HR leading to reduced microbial eukaryotic diversity in low activity sediments. The patchy nature of organic matter fluxes (Gooday, 2002) would also be consistent with the enhanced variability in diversity among North HR low activity sites.

Oxygen adds another level of complexity because South HR is located within the OMZ, but more comparative studies between seep regions at different depths and with different oxygen conditions are needed. Our observations are consistent with previous studies showing that microbial eukaryotes exhibit higher diversity in low oxygen systems (Behnke *et al.*, 2006, 2010; Forster *et al.*, 2012) compared to the surrounding oxygenated habitats. These patterns differ from those of foraminifera as well as macro- and megafauna which exhibit decreased richness in low oxygen habitats (Levin *et al.*, 2001; Levin, 2003; Gooday *et al.*, 2009, 2010). Both reduced inputs of surface production and low oxygen would act to increase microbial eukaryotic diversity at South HR, consistent with what we observed.

Ecology of Microbial Eukaryotes at Hydrate Ridge

Ciliates were the dominant sequences recovered in clone libraries from three different depths of a microbial mat (Fig. S2). This finding is consistent with previous studies of protistan communities in microbial mats from deep-sea methane seeps (Takishita *et al.*, 2010) as well as the suboxic waters and anoxic sediments from other habitats, including an anoxic basin

(Edgcomb *et al.*, 2011c), hydrothermal vent (Coyne *et al.*, 2013), salt marsh (Stoeck and Epstein, 2003) and anoxic fjord (Behnke *et al.*, 2010). These sequence-based results are also supported by independent microscopy surveys of a methane seep in Monterey Bay, showing a high abundance of ciliates in active seep sediments relative to the surrounding deep sea sediments (Buck and Barry, 1998). It is important to note that ciliates were not the most abundant group of organisms in the iTAG data. However, this is likely an artifact of deep-sequencing detecting remnant DNA from organisms originating from the photic zone that are no longer viable in seep sediments (e.g., e-DNA; Pawlowski *et al*., 2011) and/or primer differences (Stoeck *et al.*, 2010; 2014) (see supplemental material for a more detailed discussion).

Sequences were identified from eleven described ciliate classes, and their distributions in relationship to depth and sulfide (from both the clone library and iTAG data) are not only consistent between data sets, but are also consistent with what is known about their ecologies from similar habitats (Fig. 4). For example, Plagiopyleans are either anaerobic or microaerophilic, known to live in or above sulfide-containing sediments, and thought to feed predominantly on sulfur-oxidizing bacteria (Fenchel, 1968; Schulz *et al.*, 1990; Lynn, 2008). Therefore, the higher abundance of Plagiopylean ciliates in low to moderate sulfide ranges and their decrease in abundance with increasing sulfide (and decreasing oxygen) is likely related to availability of their sulfur-oxidizing prey. The greater abundance of two other ciliate groups, the Armophorea and Litostomatea, within high sulfide sediments (9-12 mM) is likely related to a combination of food availability as well as their ability to adapt to an anoxic lifestyle. Armophorea (e.g., *Caenomorpha)*, while globally distributed, are physiologically restricted to anoxic habitats (Lynn, 2008) and have been reported to have slow growth rates and require high concentrations of bacterial prey for survival (Guhl and Finlay 1993). Haptorians, a group of

475 ciliates within the Litostomatea, are also often reported from anoxic sediments (Guhl *et al.*,
476 1996; Madoni and Sartore, 2003) and are known to feed on other protists (flagellates and ciliates)
477 and even small metazoans (reviewed in Lynn, 2008). Oligohymenophoreans exhibited high
478 relative abundances across all sulfide levels, but peaked at the highest sulfide levels (12-15 mM).
479 Scutiociliates, the dominant group within the Oligohymenophoreans, are typically
480 microphagus bacterivores that live at or below the oxycline (Fenchel *et al.*, 1990). However,
481 these ciliates are also often the first to become associated with sinking detritus on which bacteria
482 are growing (Silver *et al.*, 1984). Therefore, the high overall abundance and OTU richness of
483 Oligohymenophoreans in the present sediment samples may reflect both active seep-associated
484 ciliates as well as exogenous organisms attached to sinking particles from the water column.
485 A portion of the ciliate diversity we observed occurred within clades found only in other
486 reducing ecosystems (Figs. 3, 4). A number of sequences from all three clone libraries as well as
487 sequences from the iTAG data fell into the recently described Novel Seep Clade (Takishita *et al.*,
488 2010). This clade is comprised only of sequences from other anoxic environments, including
489 microbial mat surface sediments from other seep habitats as well as hydrothermal vents (Buck *et*
490 *al.*, 2009; Takishita *et al.*, 2010; Coyne *et al.*, 2013). Determining whether this clade represents a
491 new class or falls within the Colpodea is beyond the scope of this study. However, Colpodeans
492 are known to form cysts (Lynn, 2008; Weiss *et al.*, 2013). Therefore, if species within this clade
493 exhibit the same strategies as other Colpodean ciliates, these organisms may be well suited to
494 handle the ephemeral nature of deep-sea seeps. Sequences for Cariacotrichea, another new class
495 of ciliates, were most abundant at higher sulfide concentrations (~9-15 mM). This group is
496 thought to contain species restricted to anoxic marine environments, such as the Cariaco Basin
497 (Orsi *et al.*, 2011; 2012a). Perhaps this group has adaptations that give it a competitive advantage

498 in anoxic, highly sulfidic environments such as seep sediments and responds to high levels of
499 prey much like the Armophorea and Litostomatea.
500 Other groups of protists that exhibited variability in response to the environmental
501 heterogeneity at seeps include the Cercozoa, Foraminifera and Amoebozoa. Within the
502 Cercozoa, Novel Clade 12 is thought to be a marine clade and sequences belonging to this clade
503 have been exclusively found at low oxygen and/or deep-sea sites (Bass *et al*., 2009). The higher
504 abundance of this clade in the sediments relative to carbonates may be related to its optimal
505 growth conditions. However, other Cercozoan clades appear to have different habitat
506 preferences. The sequences we recovered from the Chlorarachnea all belonged the LC104-
507 lineage, which was first recovered from the Lost City hydrothermal vent carbonates (Lopez-
508 Garcia *et al.,* 2007). Strong habitat preferences among different clades within the Cercozoa at
509 seeps are likely related to the diverse morphologies (e.g., gliding zooflagellates and filose
510 amoebae) exhibited within this Phylum (Bass and Cavalier-Smith, 2004; Howe *et al.,* 2011).
511 Within the Amoebozoa, Breviatea is a more recently established class (Cavalier-Smith *et al.*,
512 2004) that contains putatively anaerobic organisms. Aside from *Mastigamoeba invertens*,
513 sequences in this group have only been recovered from environmental DNA sequencing
514 (Dawson and Pace 2002; Cavalier-Smith *et al.,* 2004). The higher abundance of Breviatea in
515 active sediments, particularly microbial mats, is consistent with an anaerobic lifestyle. Benthic
516 foraminifera are one of the most abundant and diverse groups of protists in deep-sea sediments
517 (Lecroq *et al.* 2011; Todo *et al*., 2005). However, the cosmopolitan nature of foraminifera
518 suggests this group of organisms is not endemic to seeps (e.g., Rathburn *et al*., 2000; Burkett *et*
519 *al*., 2014). While the foraminifera, particularly the monothalamids, were abundant and diverse in
520 low activity sediments and carbonates, they were almost entirely absent from active seep

sediments during our study. Characterizing the structure of microbial eukaryotic communities in response to varying environmental conditions and relating microbial eukaryotic ecologies to their distributions are key steps towards understanding how microbial eukaryotes influence seep ecosystem function, but more comparative studies, coupled to *in situ* experimentation, are needed.

Experimental Procedures

Sample collection and pore-water analyses

Samples were collected from North HR (44° 40' N, 125° 06' W; 590 m) and South HR (44° 34' N, 125° 09' W; 800 m) offshore of Newport OR, USA during R/V *Atlantis* cruise 18-10 (29 August-9 September 2011) using the ROV *JASON*. Push cores were used to collect sediment from clam beds (n=4; 3 from North HR, 1 from South HR), white microbial mats (n=5; 2 from North HR, 3 from South HR) and low activity sediment habitats (n=3; 2 from North HR, 1 from South HR; Fig. 1). Carbonates were also collected from active (n=10) and low activity reference (n=8) sites (15 from North HR; 3 from South HR; Fig. 1). Low activity sites refer to areas adjacent to active seeps that lack diagnostic indicators of significant activity (e.g., bubbling, visible mats). At sea, carbonates were subsampled immediately after collection. Sediment cores were sectioned into 3-cm intervals (0-3, 3-6 and 6-9 cm) as described in Orphan *et al.* (2004), and sub-samples were taken directly from each fraction for molecular analyses of the microbial eukaryotic community (18S rRNA gene clone libraries, T-RFLP fingerprinting and iTAG sequencing) and geochemistry. Sub-samples for molecular work were frozen immediately and maintained at -80°C until further processing in the laboratory. Pore waters used for the analysis

544 of dissolved hydrogen sulfide (HS^-) were collected using rhizons (Rhizosphere Research
545 Products) from the same cores in which the microbial eukaryotic community was examined.
546 Sediment from each depth interval was scooped into 15-mL centrifuge tubes. Acid-washed
547 rhizons were then inserted into the sediment, and the entire set-up was kept at 4°C under
548 anaerobic conditions (mylar bags with Ar or N_2 headspace) for approximately 24 hr. 200 µl of
549 the extracted pore water was then added to 200 µl of 0.5 M zinc acetate and stored at room
550 temperature until measured using a colorimetric assay (Cline 1969). Dissolved sulfate (SO_4^{2-}),
551 concentrations were determined using pore waters from paired cores collected adjacent to the
552 cores in which the microbial eukaryotic communities were examined. Pore waters were squeezed
553 from each 3-cm sediment interval using a pressurized gas sediment Reeburgh-style squeezer (KC
554 Denmark A/S; Reeburgh 1967), and samples were collected into attached air-tight 60-ml
555 disposable syringes. Sulfate concentrations were obtained by ion chromatography (Dionex DX-
556 100).
557
558 *DNA extraction and PCR amplification for 18S rRNA clone libraries and T-RFLP*
559 In the laboratory, DNA was extracted from each sediment horizon using a Power Soil
560 DNA Extraction Kit (MO BIO Laboratories, Carlsbad, CA). For clone libraries and T-RFLP,
561 full-length eukaryotic 18S rRNA genes (optimally 1800 bp) were amplified using the general
562 eukaryotic primers MoonA (ACCTGGTTGATCCTGCCAG) and MoonB
563 (TGATCCTTCYGCAGGTTCAC) (Moon-van der Staay *et al.*, 2000; Takishita *et al.*, 2010).
564 PCR reagents were mixed at the following final concentrations: 0.5 µM of each primer, 1X PCR
565 buffer (New England BioLabs, Inc), 1.5 mM MgCl2 (NEB), 0.25 mM dNTPs (NEB), 2.5 U of
566 Taq (NEB), and 50 ng of DNA template. The PCR thermal protocol (modified from Medlin *et*

567 *al.*, 1988) was 1 min at 95°C followed by 35 cycles of: 30 sec at 95°C (denaturation), 30 sec at
568 57°C (annealing), and 2 min at 72°C (extension), with a final elongation step of 7 min at 72°C
569 and a final holding of 4°C. The amplicons were visualized on a 1% agarose gel.
570
571 *Clone library construction, phylogenetic analysis and in-silico digestion*
572 A microbial mat core from North HR was used for clone library construction in order to
573 characterize the eukaryotic community based on the full-length 18S rRNA gene. Amplicons
574 were cloned using the TOPO TA cloning kit according to the instructions of the manufacturer
575 (Life Technologies, CA). 192, 96 and 96 clones were picked from the 0-3, 3-6 and 6-9 cm
576 horizons, respectively. Screening for the libraries was conducted by restriction fragment length
577 polymorphism (RFLP) analysis on M13F- and M13R-amplfied products using both *Hae*III and
578 *Bst*UI restriction enzymes (NEB). Unique clones were identified from their restriction pattern
579 and amplicons were purified using a MultiScreen Plate (EMD Millipore). 96, 61 and 21 unique
580 amplicons from 0-3, 3-6 and 6-9 cm horizons were sent for sequencing. Inserts were sequenced
581 bi-directionally by Laragen (Culver City, CA) using an AB3730XL instrument with internal T3
582 and T7 primers. Sequences were manually trimmed and edited in Sequencher (Gene Codes
583 Coporation, MI). Contigs were assembled when possible, otherwise partial sequences (~900 bp)
584 were used for further analysis. The sequences were checked for chimeras using UCHIME
585 (www.drive5.com). Sequences were aligned to a reference alignment using the SILVA
586 Incremental Aligner (SINA) (Pruesse 2012). BLAST (Altschul 1990) was used to determine the
587 coarse phylogenetic identity of each 18S rRNA ribotype (e.g., protistan, metazoan, or fungi), and
588 the relative proportion of each type of clone within each library was estimated from their RFLP
589 patterns. In order to quantify how diversity estimates based on 18S rRNA gene sequencing

compared to T-RFLP diversity estimates, *in silico* digestion was performed on each OTU within the clone libraries using *Hae*III (GG'CC) and *Bst*UI (CG'CG) restriction enzymes. Sequences were aligned to a reference alignment using the SILVA Incremental Aligner (SINA) (Pruesse 2012). BLAST (Altschul 1990) was used to determine the coarse phylogenetic identity of each 18S rRNA ribotype (e.g., protistan, metazoan, or fungi), and the relative proportion of each type of clone within each library was estimated from their RFLP patterns. After removal of potential chimeras, archaeal, fungal and metazoan sequences, the remaining protistan sequences were imported into the ARB software package (http://www.arb-home.de/) and incorporated into the existing eukaryotic tree (SILVA SSU database release 111) using the parsimony add tool (Ludwig *et al.*, 2004). The protistan lineages in this version of SILVA have been reconciled with the recommendations outlined in Adl *et al.*, (2005) and further improved by the most recent recommendations from the ISOP committee in Adl *et al.* (2012). Sequences were grouped into operational taxonomic units (OTUs) based on 98% sequence similarity. The phylogenetic identity of the non-ciliate protistan sequences was determined based on their placement on the reference tree. A maximum likelihood phylogeny of ciliate sequences was constructed using RAxML 7.2.8 (Stamatakis, 2006) with 1000 rapid bootstrap inferences and GTRGAMMA rate approximation. Sequences of protistan OTUs obtained from this study have been deposited in GenBank with accession numbers KT346251 to KT346331.

Transcription Fragment Length Polymorphism (T-RFLP) fingerprinting and data analysis

To characterize the microbial eukaryotic community using T-RFLP fingerprinting, each sediment sample was extracted and amplified in replicate (34 samples from 12 cores x 3 depth horizons, except that 2 cores did not have a 6-9 cm depth horizon) using the same PCR primers

as used for clone library construction. Carbonate samples were excluded from T-RFLP analysis (see supplemental material for additional details). Following the first PCR amplification (described above), 5 µL of the original PCR product was amplified in a 25 µl PCR reaction with PuReTaq Ready-To-Go PCR beads (GE Healthcare). For this, we used the same primers as in the original PCR, but the MoonA primer was modified with a 6-FAM fluorescent dye on the 5' end. PCR was performed using the same thermal cycling protocol as the original PCR, but run for 15-20 cycles to obtain approximately 125 ng of DNA (quantified on a gel using a 1 kb ladder, New England BioLabs). The PCR product was digested with both *Hae*III and *Bst*UI. Restriction enzymes for this study were chosen based on *in silico* digestion of publically available protistan sequences from similar environments to provide a combination of phylogenetic resolution and fragment lengths that were within the range of fragments analyzed using the ABI sequencer. Fragment analysis was done by Laragen (Culver City, CA) using an AB3730XL. Additional details for the fragment analysis, data processing and quality control are provided in supplemental material.

PCR amplification and Illumina massively-parallel, high-throughput tag sequencing (iTAG)

The same DNA extracts used for T-RFLP were used for iTAG sequencing. To characterize the eukaryotic community based on short-read, high-throughput sequencing of the 18S rRNA gene, the V9 region was amplified using 1391F (5'-GTACACACCGCCCGTC-3') (Lane 1991) and EukB (5'-TGATCCTTCTGCAGGTTCACCTAC-3') (Medlin *et al.*, 1988) (resulting in ~150 bp amplicons. The 1391F primer is a highly conserved universal primer (e.g., potential for amplifying non-eukaryotic organisms; Stock et al., 2009), as opposed to the Amaral-Zettler et al. (2009) primer which was designed specifically to avoid amplification of

636 eukaryotic sequences but also misses some higher-taxon prokaryote groups. We applied the
637 1391F primer because the depth of Illumina sequencing allowed us to filter out eukaryotic
638 sequences and still retain a robust dataset. While the V9 18S rRNA hypervariable region alone
639 does not discriminate at the species level (Stoeck *et al.*, 2010, Amaral-Zettler 2013), the V9
640 region allows for a relatively unbiased broad comparison of eukaryotic diversity in
641 underexplored habitats.

642 We followed the Earth Microbiome Project (EMP; Gilbert *et al.*, 2011) recommended
643 protocol (Caporaso *et al.*, 2011, 2012), but implemented the Illumina 2-step PCR method for
644 amplification (www.illumina.com). Primers were modified with Illumina adaptors in the first
645 PCR step (Fig. S1) and barcoded indices (P5/P7 indices; Fig. S1) were added during the second
646 PCR step in order to minimize PCR bias by employing long primers over many cycles (Berry *et*
647 *al.*, 2011). The PCR protocol for V9 amplification employed an initial activation step at 95 °C
648 for 2 min, followed by 30 cycles consisting of 95 °C for 30 s, 57 °C for 30 s, and 72 °C for 90
649 sec; and a final 10-min extension at 72 °C. For the second PCR step, 5 μL of the amplicon
650 product from the first PCR was used as template in a 10 cycle, 25 μL reconditioning reaction
651 with the same PCR conditions, but using the barcoded primers. The same 34 sediment samples
652 that were used for T-RFLP analysis as well as 13 carbonate samples were amplified in duplicate.
653 After all PCR reactions were completed, duplicate barcoded products were pooled and quantified
654 with a Qubit fluorometer (Thermo Fisher Scientific). Barcoded amplicons were mixed together
655 in equimolar amounts and purified in bulk through a QIAquick PCR Purification kit (Qiagen).
656 All PCR steps, amplification success and purity were checked by gel electrophoresis.

657 Paired-end 2x250 basepair sequencing was performed at Laragen, Inc (Los Angeles, CA)
658 on an Illumina MiSeq platform. At Laragen, the raw data were demultiplexed and sequences that

had >1 basepair mismatch on the 12-basepair barcode were removed. The sequence data are available in the Sequence Read Archive under accession number SRP061572. The sequences were processed in-house using QIIME1.8.0 (Caporaso *et al.*, 2010) according to the protocol outlined in Mason *et al.* (2015), with modifications related to OTU binning and taxonomy assignments. After initial quality control steps (e.g., assembly, trimming and chimera checking), 5 sediment samples (4 of which were from the 6-9 cm horizon in microbial mats) and 1 carbonate sample were removed from further analyses due to poor read recovery. Sequences from the remaining samples were used to pick de novo operational taxonomic units (OTUs) at 98% similarity. Singleton OTUs were removed from the data set and the default QIIME1.8.0 algorithm for taxonomic assignments was used against representative sequences from each OTU (Wang *et al.*, 2007). Taxa were assigned using the PR2 database (Guillou *et al.*, 2013). OTUs that were left unassigned as well as OTUs that were identified as non-microbial eukaryotes (e.g., archaeal, bacterial and metazoan sequences) were removed from the data set. Each sample was normalized to its sequence total, OTUs appearing at less than 0.01% relative abundance across the entire data set were removed in order to minimize spurious sequencing products, and the samples were renormalized. At this point, two data sets were generated and explored further using multivariate approaches. One data set included all microbial eukaryotic OTUs (98% OTU clustering; referred to throughout the text as iTAG-OTU) and the other data set included class level data for each sample (referred to throughout the text as iTAG-L4; note class level is also referred to as the fourth level of rank in the recent classification of microbial eukaryotes by Adl *et al.*, 2005, 2012). Due to the short length of the V9 region and sequence similarity used for taxonomic assignments (90%), for reliability we only assigned taxonomic labels to the class level. Furthermore, since T-RFLP resolves taxonomic differences at approximately the class

682 level (see supplemental material for more details), this level of taxonomic clustering provides the
683 best comparison between the T-RFLP and iTAG data sets. However, all multidimensional
684 analyses were done on both the iTAG-OTU and iTAG-L4 data. For alpha diversity calculations
685 [Richness (S) and Shannon Diversity (H')], each sample was rarefied to equal depth (661
686 sequences) to account for variations in sampling effort.
687
688 *Multivariate Analysis*
689 In order to compare microbial eukaryotic community composition among samples, we
690 used a series of multidimensional analyses. All statistical analyses were performed in PRIMER
691 v6 with PERMANOVA+ add-on software (PRIMER-E Ltd.). Bray-Curtis similarity was used as
692 the resemblance measure on fourth-root-transformed data. Nonmetric multidimensional scaling
693 (MDS) was used to visualize the microbial eukaryotic community composition data. Analysis of
694 similarities (ANOSIM) was used to determine the significance of between-group differences in
695 community structure (i.e., region [north vs. south], substrate [sediment vs. carbonate], habitat
696 [carbonates, microbial mats, clam beds and inactive sediments], activity [inactive vs. active],
697 sediment depth, and sulfide concentration). In order to examine the significance of sulfide
698 concentration on microbial eukaryotic composition and diversity, samples were binned into
699 sulfide ranges: 0, 0-3, 3-6, 6-9, 9-12, 12-15, >15 mM of sulfide. SIMPER was used to determine
700 if the individual taxonomic groups were associated with the overall (dis)similarity between
701 samples or within groups. Model 1 linear regression analysis was used to analyze relationships
702 between microbial eukaryotic diversity (richness) and environmental variables.
703

Acknowledgements

We are grateful to the captain and crew of the R/V *Atlantis* and the *JASON* pilots who helped make sampling possible. We offer thanks to J. Marlow, A. Dekas, A. Green-Saxena, S. Connon and many others for help at sea and/or in the laboratory. In particular, we would like to thank R. Leon for help developing at-sea methods, J. Glass for providing sulfide data, G. Chadwick, E. Wilbanks and C. Skennerton for programming assistance, G. Mendoza for helpful input regarding the statistical analyses and E. Allen for insightful discussions about sample processing and analyses. Support for this research was provided by grant OCE 0825791, OCE 0826254 and OCE 0939557 from the US National Science Foundation (NSF). VJO supported by a grant from the Gordon and Betty Moore Foundation Marine Microbial Initiative (GBMF3780). NSF Graduate Research Fellowships supported ALP and DHC, and a P.E.O Scholar Award additionally supported ALP.

References

Adl, S.M., Habura, A., and Eglit, Y. (2014) Amplification primers of SSU rDNA for soil protists. Soil Biol Biochem. 69: 328-342.

Adl, S.M., Simpson, A.G.B., Farmer M.A., Andersen, R.A., Anderson, O.R., Barta, J.R., *et al.* (2005) The new higher level classification of eukaryotes with emphasis on the taxonomy of protists. J Eukaryot Microbiol 52: 399-451.

Adl, S.M., Simpson, A.G.B., Lane, C.E., Lukes, J., Bass, D., Bowser, S.S., *et al.* (2012) The revised classification of eukaryotes. J Eukaryot Microbiol 59:429-493.

Aloisi, G., Bouloubassi, I., Heijs, S.K., Pancost, R.D., Pierre, C., Sinninghe Damsté, J.S., *et al.* (2002) CH4-consuming microorganisms and the formation of carbonate crusts at cold seeps. Earth Planet Sci Lett 203:195-203.

Aloisi, G., Wallmann, K., Haese, R., and Saliége, J.-F. (2004) Chemical, biological and hydrological controls on the 14C content of cold seep carbonate crusts: numerical modeling and implications for convection at cold seeps. Chem Geol 213: 359-383.

Altschul, S.F., Gish, W., Miller, W., Myers, E.W., and Lipman, D.J. (1990) Basic local alignment search tool. J Mol Biol 215: 403-410.

Amaral-Zettler, L.A. (2013) Eukaryotic diversity at pH extremes. Front Microbiol 441:1-17.

Amaral-Zettler, L.A., McCliment, E.A., Ducklow, H.W., and Huse, S.M. (2009) A method for studying protistan diversity using massively parallel sequencing of V9 hypervariable regions of small-subunit ribosomal RNA genes. PLOS One 4:7:e6372.

Anderson, R., Winter, C., and Jürgens, K. (2012) Protist grazing and viral lysis as prokaryotic mortality factors at the Baltic Sea oxic-anoxic interfaces. Mar Ecol Prog Ser 467: 1-14.

Anderson, R., Wylezich, C., Glaubitz, S., Labrenz, M., and Jürgens, K. 2013. Impact of protist grazing on a key bacterial group for biogeochemical cycling in the Baltic Sea pelagic oxic/anoxic interfaces. Environ Microbiol 15: 1580-1594.

Bass, D., Chao, E.E.Y., Nikolaev, S., Yabuki, A., Ishida, K., Berney, C., *et al*. (2009) Phylogeny of Novel Naked Filose and Reticulose Cercozoa: Granofilosea cl. n. and Proteomyxidea Revised. Protist 160: 75-109.

746 Bass, D., and Cavalier-Smith, T. (2004) Phylum-specific environmental DNA analysis reveals
747 remarkably high global biodiversity of Cercozoa (Protozoa). Int J Syst Evol Microbiol 54:
748 2393-2404.

749 Behnke, A., Bunge, J., Barger, K., Breiner, H-W., Alla, V., and Stoeck, T. (2006)
750 Microeukaryote community patterns along an O2/H2S gradient in a supersulfidic anoxic
751 fjord (Framvaren, Norway). Appl Environ Microbiol 72: 3626-3636.

752 Behnke, A., Barger, K., Bunge, J., and Stoeck, T. (2010) Spatio-temporal variations in protistan
753 communities along an O_2/H_2S gradient in the anoxic Framaren Fjord (Norway). FEMS
754 Microbiol Ecol 72: 89-102.

755 Berry, D., Mahfoudh, K.B., Wagner, M., and Loy, A. (2011) Barcoded primers used in multiplex
756 amplicon pyrosequencing bias amplification. Appl Environ Microbiol 77: 7846–7849.

757 Boetius, A., Ravenschlag, K., Schubert, C.J., Rickert, D., Widdel, F., Gieseke, A., *et al.* (2000) A
758 marine microbial consortium apparently mediating anaerobic oxidation of methane. Nature
759 407: 623-626.

760 Boetius, A., and Suess, E. (2004) Hydrate Ridge: a natural laboratory for the study of microbial
761 life fueled by methane from near-surface gas hydrates. Chemical Geology 205: 291-310.

762 Buck, K.R. and Barry, J.P. (1998) Monterey Bay cold seep infauna: quantitative comparison of
763 bacterial mat meiofauna with non-seep control sites. Cah Biol Mar 39: 333-335.

764 Buck, K.R., Barry, J.P., and Hallam, S.J. (2009) Microbial assemblages associated with
765 Thioploca sheaths from cold seep settings in Monterey. Accession #: FJ814761.
766 Unpublished.

767 Buck, K.R., Barry, J.P., and Simpson, A.G.B. (2000) Monterey Bay cold seep biota: euglenozoa
768 with chemoautotrophic bacterial epibionts. Europ J Protistol 36: 117-126.

769 Burkett, A.M., Rathburn, A.E., Perez, M.E., Levin, L.A., Cha, H., and Rouse, G.W. (2015)
770 Phylogenetic placement of *Cibicidoides wuellerstorfi* (Schwager, 1866) from methane seeps
771 and non-seep habitats on the Pacific margin. Geobiology 13: 44-52.

772 Calbet, A., and Landry, M.R. (2004) Phytoplankton growth, microzooplankton grazing and
773 carbon cycling in marine systems. Limnol Oceanogr 49: 51-57.

774 Caporaso, J.G., Kuczynski, J., Stombaugh, J., Bittinger, K., Bushman, F.D., Costello, E.K., *et al.*
775 (2010) QIIME allows analysis of high-throughput community sequencing data. *Nat Methods*
776 7: 335-336.

777 Caporaso, J.G., Lauber, C.L., Walters, W.A., Berg-Lyons, D., Lozupone, C.A., Tumbaugh, P.J.,
778 *et al.* (2011) Global patterns of 16S rRNA diversity at a depth of millions of sequences per
779 sample. PNAS 108: 4516-4522.

780 Caporaso, J.G., Lauber, C.L., Walters, W.A., Berg-Lyons, D., Huntley, J., Fierer, N., *et al.*
781 (2012) Ultra-high-throughput microbial community analysis on the Illumina HiSeq and
782 MiSeq platforms. ISME J 6: 1621-1624.

783 Cavalier-Smith, T., Chao, E.E.Y., and Oates, B. (2004) Moleculary phylogeny of Amoebozoa
784 and the evolutionary significance of the unikont *Phalansterium*. Europ J Protistol 40: 21-48.

785 Cline, J. (1969) Spectrophotometric determination of hydrogen sulphide in natural waters.
786 Limnol Oceanogr 14:454-458.

787 Cordes, E.E., Cunha, M.R., Galeron, J., Mora, C., Roy, K.O., Myriam, S., *et al.* (2009) The
788 influence of geological, geochemical, and biogenic habitat heterogeneity on seep
789 biodiversity. Mar Ecol 31: 51-65.

790 Coyne, K.J., Countway, P.D., Pilditch, C.A., Lee, C.K., Caron, D.A., and Cary, S.C. (2013)
791 Diversity and distributional patterns in ciliates in Guaymas Basin hydrothermal vent
792 sediments. J Eukaryot Microbiol 60: 433-447.

793 Dando, P.R., Austen, M.C., Burke, R.A., Kendall, M.A., Kennicutt, M.C., Judd, A.G., *et al.*
794 (1991) Ecology of a North Sea pockmark with an active methane seep. Mar Ecol Prog Ser
795 70: 49-63.

796 Dando, P.R., Bussmann, I., Niven, S.J., O'Hara, S.C.M., Schmaljohann, L.J., Taylor, *et al.*
797 (1994) A methane seep area in the Skagerrak, the habitat of the pogonophore *Siboglinum*
798 *poseidoni* and the bivalve mollusc *Thyasira sarsi*. Mar Ecol Prog Ser 107: 157-167.

799 Dawson, S.C., and Pace, N.R. (2002) Novel kingdom-level eukaryotic diversity in anoxic
800 environments. Proc Natl Acad Sci 99: 8324-8329.

801 Dorst, J., Bissett, A., Palmer, A.S., Brown, M., Snape, I., Stark, J.S., *et al.* (2014) Community
802 fingerprinting in a sequencing world. FEMS Microbiol Ecol 2: 316-330.

Edgcomb, V.P., Kysela, D.T., Teske, A., de Vera Gomez, A., and Sogin, M.L. (2002) Benthic eukaryotic diversity in the Guaymas Basin hydrothermal vent environment. PNAS 99: 7658-7662.

Edgcomb, V., Orsi, W., Leslin, C., Epstein, S.S., Bunge, J., Jeon, S., *et al.* (2009) Protistan community patterns within the brine and halocline of deep hypersaline anoxic basins in the eastern Mediterranean Sea. Extremophiles 13: 151-167.

Edgcomb, V.P., Breglia, S.A., Yubuki, N., Beaudoin, D., Patterson, D.J., Leander, B.S., and Bernhard, J.M. (2011a) Identity of epibiotic bacteria on symbiontid euglenozoans in O_2-depleted marine sediments: evidence for symbiont and host co-evolution. ISME J 5: 231-243.

Edgcomb, V.P., Leadbetter, E.R., Bourland, W., Beaudoin, D., and Bernhard, J.M. (2011b) Structured multiple endosymbiosis of bacteria and archaea in a ciliate from marine sulfidic sediments: a survival mechanism in low oxygen, sulfidic sediments? Front Microbiol doi:10.3389/fmicb.2011.00055.

Edgcomb, V.P., Orsi, W., Bunge, J., Jeon, S., Christen, R., Leslin, C., *et al.* (2011c) Protistan microbial observatory in the Cariaco Basin, Caribbean. I. Pyrosequencing vs Sanger insights into species richness. ISME J 5: 1344-1356.

Fenchel, T. (1968) The ecology of marine microbenthos. II. The food of marine benthic ciliates. Ophelia 5: 73-121.

Fenchel, T., and Finlay, B.J. (1990a) Anaerobic free-living protozoa: growth efficiencies and the structure of anaerobic communities. FEMS Microbiol Ecol 74: 269-276.

Fenchel, T., and Finlay, B.J. (1990b) Oxygen toxicity, respiration and behavioral responses to oxygen in free-living anaerobic ciliates. J Gen Microbiol 136: 1953-1959.

Fenchel, T., and Finlay, B.J. (1991) The biology of free-living anaerobic ciliates. Europ J Protistol 26: 201-215.

Fenchel, T., and Finlay, B.J. (1995) Ecology and evolution in anoxic worlds. University Press, Oxford.

Fenchel, T., Kristensen, L.D., and Rasmusen, L. (1990) Water column anoxia: vertical zonation of planktonic protozoa. Mar Ecol Prog Ser 62: 1-10.

Finlay, B.J., Fenchel, T., and Gardener, S. (1986) Oxygen perception and O_2 toxicity in the freshwater ciliated protozoan *Loxodes*. Protozool 33:157-165.

833 Forster, D., Behnke, A., and Stoeck, T. (2012) Meta-analyses of environmental sequence data
834 identify anoxia and salinity as parameters shaping ciliate communities. Syst Biodivers 10:
835 277-288.

836 German, C.R., Ramirez-Llodra, E., Baker, M.C., Tyler, P.A., and the ChEss Scientific Steering
837 Committee. (2011) Deep-water chemosynthetic ecosystem research during the census of
838 marine life decade and beyond: a proposed deep-ocean road map. PLOS One 6:e23529.

839 Gieskes, J., Mahn, C., Day, S., Martin, J.B., Greinert, J., Rathburn, T., and McAdoo, B. (2005) A
840 study of the chemistry of pore fluids and authigenic carbonates in methane seep
841 environments: Kodiak Trench, Hydrate Ridge, Monterey Bay, and Eel River Basin. Chem
842 Geol 220: 329-345.

843 Gilbert, J.A., Meyer, F., Jansson, J., Gordon, J., Pace, N. Tiedje, J., *et al.* (2011) The Earth
844 Microbiome Project: Meeting report of the "1st EMP meeting on sample selection and
845 acquisition" at Argonne National Laboratory October 6th 2010 1-5.

846 Gong, J., Dong, J., Liu, X., Massana, R. (2013) Extremely high copy numbers and
847 polymorphisms of the rDNA operon estimated from single cell analysis of Oligotrich and
848 Peritrich ciliates. Protist 164: 369-379.

849 Gooday, A.J. (2002) Biological responses to seasonally varying fluxes of organic matter to the
850 ocean floor: a review. J Oceanogr 58: 305-332.

851 Gooday, A.J., Hughes, J.A., and Levin, L.A. (2001) The foraminiferan macrofauna from three
852 North Carolina (USA) slope sites with contrasting carbon flux: a comparison with metazoan
853 macrofauna. Deep-Sea Res I 48: 1709-1739.

854 Gooday, A.J., Levin, L.A., da Silva, A.A., Bett, B.J., Cowie, G.L., Dissard, D., *et al.* (2009)
855 Faunal responses to oxygen gradients on the Pakistan margin: a comparison of
856 foraminiferans, macrofauna and megafauna. Deep-Sea Res II 56: 488-502.

857 Gooday, A.J., Bett, B.J., Escobar, E., Ingole, B., Levin, L.A., Neira, C., *et al.* (2010) Habitat
858 heterogeneity and its relationship to biodiversity in oxygen minimum zones. Mar Ecol 31:
859 125-147.

860 Guhl, B.E., and Finlay, B.J. (1993) Anaerobic predatory ciliates track seasonal migrations of
861 planktonic photosynthetic bacteria. FEMS Microbiol Let 107: 313-316.

Guhl, B.E., Finlay, B.J., and Schink, B. (1996) Comparisons of ciliate communities in the anoxic hypolimnia of three lakes: general features and the influence of lake characteristics. J Plankton Res 18: 335-353.

Guilini, K., Levin, L.A., and Vanreusel, A. (2012) Cold seep and oxygen minimum zone associated sources of margin heterogeneity affect benthic assemblages, diversity and nutrition at the Cascadia margin (NE Pacific Ocean). Prog Oceanogr 96: 77-92.

Guillou, L., Bachar, D., Audic, S. Bass, D., Berney, C., Bittner, L., *et al.* (2013) The Protist Ribosomal Reference database (PR2): a catalog of unicellular eukaryote Small Sub-Unit rRNA sequences with curated taxonomy. Nuc Acids Res 41: 597-604.

Helly, J.J., and Levin, L.A. (2004) Global distribution of naturally occurring marine hypoxia on continental margins. Deep-Sea Res I 51: 1159-1168.

Howe, A.T., Bass, D., Scoble, J.M., Lewis, R., Vickerman, K., Arndt, H., Cavalier-Smith, T. (2011) Novel cultured protists identifying deep-branching environmental DNA clades of Cercozoa: new Genera *Tremula, Micrometopion, Minimassisteria, Nudifila, Peregrinia*. Protist 162:332-372.

Kerr, S.R. (1977) Theory of size distribution in ecological communities. J Fish Res Board Can 31: 1859-1862.

Knittle, K., and Boetius, B. (2009) Anaerobic oxidation of methane: progress with an unknown process. Annu Rev Microbiol 63: 311-334.

Kunin,V., Engelbrektson, A., Ochman, H., Hugenholtz, P. (2010). Wrinkles in the rare biosphere: pyrosequencing errors can lead to artificial inflation of diversity estimates. Environ Microbiol 12: 118-123.

Lane, D.J. (1991) 16S/23S sequencing. In:Nucleic Acid Technologies in Bacterial Systematics. (eds Stackebrandt E, Goodfellow M). pp. 115-175, John Wiley and Sons Ltd., New York, NY

Lecroq, B., Lejzerowicz, F., Bachar, D., Christen, R., Esling, P. Baerlocher, L., *et al*. (2011) Ultra-deep sequencing of foraminiferal microbarcodes unveils hidden richness of early monothalamous lineages in deep-sea sediments. PNAS 108: 13177-13182.

Lee, C.K., Herbold, C.W., Polson, S.W., Wommack, K.E., Williamson, S.J., McDonald, I.R., and Cary S.C. (2012) Groundtruthing next-gen sequencing for microbial ecology-biases and

errors in community structure estimates from PCR amplicon pyrosequencing. PLoS ONE 7: e44224.

Levin, L.A. (2005) Ecology of cold seep sediments: interactions of fauna with flow, chemistry and microbes. Oceanogr Mar Biol, Annu Rev 43: 1-46.

Levin, L.A., Etter, R.J., Rex, M.A., Gooday, A.J., Smith, C.R., Pineda, J., *et al.* (2001) Environmental influences on regional deep-sea species diversity. Ann Rev Ecol Syst 32: 51-93.

Levin, L.A., and Mendoza, G. (2007) Community structure and nutrition of deep methane seep macroinfauna from the Aleutian Margin and Florida Escarpment, Gulf of Mexico. Mar Ecol 28: 131-151.

Levin, L.A., Mendoza, G.F., Gonzalez, J.P., Thurber, A.R., Cordes, E.E. (2010) Diversity of bathyal macrofauna on the northeastern Pacific margin: the influence of methane seeps and oxygen minimum zones. Mar Ecol 31: 94-110.

Levin, L.A., Mendoza, G.F., Grupe, B.M., Gonzalez, J.P., Jellison, B., Rouse, G., *et al*. (2015) Biodiversity on the rocks: macrofauna inhabiting authigenic carbonate at Costa Rica methane seeps. PLOS One doi:10.1371/journal.pone.0131080.

Levin, L.A., and Michener, R. (2002) Isotopic evidence of chemosynthesis-based nutrition of macrobenthos: the lightness of being at Pacific methane seeps. Limnol Oceanogr 47:1336-1345.

Levin, L.A., Ziebis, W., Mendoza, G.F., Growney, V.A., Tryon, M.D., Brown, K.M., *et al.* (2003) Spatial heterogeneity of macrofauna at the northern California methane seeps: influence of sulfide concentration and fluid flow. Mar Ecol Prog Ser 265: 123-139.

López-García, P., Vereshchaka, A., and Moreira, D. (2007) Eukaryotic diversity associated with carbonates and fluid-seawater interface in Lost City hydrothermal field. Environ Microbiol 9: 546-554.

Lorenz, M.G., and Wackernagel, G. (1987) Adsorption of DNA to sand and variable degradation rates of adsorbed DNA. Appl Environ Microbiol 67: 2354-2359.

Ludwig, W., Strunk, O., Westram, R., Richter, L., Meier, H., Kumar, Y., *et al.* (2004) ARB: a software environment for sequence data. Nucleic Acids Res 32:1363-1371.

Lynn, D.H. (2008) The ciliated protozoa: characterization, classification and guide to literature. 2008, Springer Science, Dordrecht, Netherlands.

Madoni, P., and Sartore, F. (2003) Long-term changes in the structure of ciliate communities in a small isolated pond. Italian Journal of Zoology 70:313-320.

Marlow, J.J., Steele, J.A., Case, D.H., Connon, S.A., Levin, L.A., and Orphan, V.J. (2014a) Microbial abundance and diversity patterns associated with sediments and carbonates from the methane seep environments of Hydrate Ridge, OR. Front Mar Sci doi: 10.3389/fmars.2014.00044

Marlow, J.J., Steele, J.A., Ziebis, W., Thurber, A.R., Levin, L.A., and Orphan, V.J. (2014b) Carbonate-hosted methanotrophy represents an unrecognized methane sink in the deep sea. Nat Comm 5:5094, doi:10.1038/ncomms6094 |

Massana, R., and Pedrós-Alió, C. (1994) Role of anaerobic ciliates in planktonic food webs: Abundance, feeding, and impact on bacteria in the field. Appl Environ Microbiol 60: 1325-1334.

Medinger, R., Nolte, V., Pandey, R.V., Jost, S., Ottenwälder, B., Schlötterer, C., et al. (2010). Diversity in a hidden world: potential and limitation of next generation sequencing for surveys of molecular diversity of eukaryotic microorganisms. Mol Ecol 19: 32-40.

Medlin, L., Elwood, H.J., Stickel, S., and Sogin, M.L. (1988) The characterization of enzymatically amplified eukaryotic 16S-like rRNA-coding regions. Gene 71:491-499.

Milkov, A.V. (2004) Global estimates of hydrate-bound gas in marine sediments: how much is really out there? Earth Sci Rev 66: 183-197.

Montagna, P.A., Bauer, J.E., Hardin, D., and Spies, R.B. (1989) Vertical distribution of microbial and meiofaunal populations in sediments of a natural coastal hydrocarbon seep. J Mar Res 47: 657-680.

Moon-van der Staay, S.Y., van der Staay, G.W.M., Guillou, L., Vaulot, D. (2000) Abundance and diversity of prymnesiophytes in the picoplankton community from the equatorial Pacific Ocean inferred from 18S rDNA sequences. Limnol Oceanogr 45: 98-109.

Murase, J., Noll, M., and Frenzel, P. (2006) Impact of protists on the activity and structure of the bacterial community in a rice field soil. Appl Environ Microbiol 72: 5436-5444.

950 Murase, J., and Frenzel, P. (2008) Selective grazing of methanotrophs by protozoa in a rice field
951 soil. FEMS Microbiol Ecol 65: 408-414.

952 Orphan, V.J., Ussler, W., Naehr, T.H., Hinrichs, K.-U., and Paull, C.K. (2004) Geological,
953 geochemical, and microbiological heterogeneity of the seafloor around methane vents in the
954 Eel River Basin, offshore California. Chem Geol 205: 265-289.

955 Orphan, V.J., Hinrichs, K.-U., Ussler, W., Paull, C.K., Taylor, L.T., Sylva, S.P., *et al.* (2001)
956 Comparative analysis of methane-oxidizing archaea and sulfate-reducing bacteria in anoxic
957 marine sediments. Appl Environ Microbiol 67:1922-1934.

958 Orsi, W., Edgcomb, V., Faria, J., Foissner, W., Fowle, W.H., Hohmann, T., *et al.* (2012a) Class
959 Cariacotrichea, a novel ciliate taxon from the anoxic Cariaco Basin, Venezuela. Int J Syst
960 Evol Microbiol 62: 1425-1433.

961 Orsi, W., Edgcomb, V., Jeon, S., Leslin, C., Bunge, J., Taylor, G.T., *et al.* (2011) Protistan
962 microbial observatory in the Cariaco Basin, Caribbean. II. Habitat specialization. ISME J 5:
963 1367-1373.

964 Orsi, W., Song, Y.C., Hallam, S., and Edgcomb, V. (2012b) Effect of oxygen minimum zone
965 formation on communities of marine protists. ISME J 6:1586-1601.

966 Pawlowski, J., Christen, R., Lecroq, B., Bachar, D., Shahbazkia, H.R., Amaral-Zettler, L., and
967 Guillou, L. (2011) Eukaryotic richness in the abyss: insights from pyrotag sequencing. PLOS
968 One 6: e18169.

969 Platt, T. and Denman, K. (1977) Organisation in the pelagic ecosystem. Helgolander wiss
970 Meeresunters 30:575-581.

971 Pilloni, G., Granitsiotis, M.S., Engel, M., and Lueders, T. (2012) Testing the limits of 454
972 pyrotag sequencing: reproducibility, quantitative assessment and comparison to T-RFLP
973 fingerprinting of aquifer microbes. PLOS One 7:e40476.

974 Pruesse, E., Peplies, J., and Glöckner, F.O. (2012) SINA: accurate high-throughput multiple
975 sequence alignment of ribosomal RNA genes. Bioinformatics 28: 1823-1829.

976 Rathburn, A.E., Levin, L.A., Held, Z., and Lohmann, K.C. (2000) Benthic foraminifera
977 associated with cold methane seeps on the Northern California Margin: ecology and stable
978 isotopic composition. Mar Micropaleontol 38: 247-266.

979 Reeburgh, W.S. (1967) An improved interstitial water sampler. Limnol Oceanogr 12: 163-165.

Ruff, S.E., Biddle, J.F., Teskes, A.P., Knittel, K., Boetius, A., and Ramette, A. (2015) Global dispersion and local diversification of the methane seep microbiome. PNAS 112: 4015-4020.

Sahling, H., Rickert, D., Lee, R.W., Linke, P., and Suess, E. (2002) Macrofaunal community structure and sulfide flux at gas hydrate deposits from the Cascadia convergent margin, NE Pacific. Mar Ecol Prog Ser 231: 121-138.

Santos, S.S., Nielsen, T.K., Hansen, L.H., and Winding, A. (2015) Comparison of three DNA extraction methods for recovery of soil protist DNA. J Microbiol Methods 115: 13-19.

Schulz, S., Wagener, S., and Pfennig, N. (1990) Utilization of various chemotrophic and phototrophic bacteria as food by the anaerobic ciliate *Trimyema compressum*. Europ J Protistol 26: 122-131.

Sherr, E.B., and Sherr, B.F. (1998) Role of microbes in pelagic food webs: a revised concept. Limnol Oceanogr 33: 1225-1227.

Sherr, E.B., and Sherr, B.F. (1994) Bacterivory and Herbivory: Key roles of phagotrophic protists in pelagic food webs. Microb Ecol 28: 223-235.

Sherr, E.B., and Sherr, B.F. (2002) Significance of predation by protists in aquatic microbial food webs. Antonie Leewenhoek Int J Gen Mol Microbiol 81: 293-308.

Silver, M.W., Gowing, M.M., Brownlee, D.C., and Corliss, J.O. (1984) Ciliated protozoa associated with oceanic sinking detritus. Nature 309: 246-248.

Sommer, S., Pfannkuche, O., Linke, P., Greinert, J., Drews, M., Gubsch, S., *et al.* (2006) Efficiency of the benthic filter: biological control of the emission of dissolved methane from sediments containing shallow gas hydrates at Hydrate Ridge. Global Biogeochem Cy doi:10.1029/2004GB002389.

Stamatakis, A. (2006) RAxML-VI-HPC: maximum likelihood based phylogenetic analyses with thousands of taxa and mixed models. Bioinformatics 22: 2688-2690.

Stock, A., Jürgens, K., Bunge, J., and Stoeck, T. (2009) Protistan diversity in the suboxic and anoxic waters of the Gotland Deep (Baltic Sea) as revealed by 18S rRNA clone libraries. Aquat Microb Ecol 55: 267284.

Stoeck, T., Bass, D., Neble, M., Christen, R., Jobes, M.D.M, Breiner, H-W. and Richards, T.A. (2010) Multiple marker parallel tag environmental DNA sequencing reveals a highly complex eukaryotic community in marine anoxic water. Molec Ecol 19: 21-31.

Stoeck, T., Behnke, A., Christen, R., Amaral-Zettler, L., Rodriguez-Mora, M.J., Chistoserdov, A., *et al.* (2009) Massively parallel tag sequencing reveals the complexity of anaerobic marine protistan communities. BCM Biology 7:72.

Stoeck, T., Breiner, H-W., Filker, S., Ostermaier, V., Kammerlander, B., and Sonntag, B. (2014). A morphogenetic survey on ciliate plankton from a mountain lake pinpoints the necessity of lineage-specific barcode markers in microbial ecology. Environ Microbiol 16: 430-444.

Stoeck, T., and Epstein, S. (2003) Novel eukaryotic lineages inferred from small-subunit rRNA analyses of oxygen-depleted marine environment. Appl Environ Microbiol 69: 2657-2663.

Straile, D. (1997) Gross growth efficiencies of protozoan and metazoan zooplankton and their dependence on food concentration, predator-prey weight ratio, and taxonomic group. Limnol Oceanogr 42: 1375-1385.

Takishita, K., Kakizoe, N., Yoshida, T., and Maruyama, T. (2010) Molecular evidence that phylogenetically diverged ciliates are active in microbial mats of deep-sea cold-seep sediment. J Eukaryot Microbiol 57: 76-86.

Takishita, K., Yubuki, B., Kakizoe, N., Inagaki, Y., and Maruyama, T. (2007) Diversity of microbial eukaryotes in sediment at a deep-sea methane cold seep: surveys of ribosomal DNA libraries from raw sediment samples and two enrichment cultures. Extremophiles 11: 563-576.

Todo, Y., Kitazato, H., Hashimoto, J., and Gooday, A.J. (2005) Simple foraminifera flourish at the ocean's deepest point. Science 307:689.

Treude, T., Boetius, A., Knittel, K., Wallmann, K., and Jørgensen, B.B. (2003) Anaerobic oxidation of methane above gas hydrates at Hydrate Ridge, NE Pacific Ocean. Mar Ecol Prog Ser 264: 1-14.

Tryon, M.D., and Brown, K.M. (2001) Complex flow patterns through Hydrate Ridge and their impact on seep biota. Geophys Res Let 28: 2863-2866.

Valentine, D.L., Blanton, D.C., Reeburgh, W.S., and Kastner, M. (2001) Water column methane oxidation adjacent to an area of active hydrate dissociation, Eel River Basin. Geochim Cosmochim Acta 65: 2633-2640.

Valentine, D.L. (2011) Emerging topics in marine methane biogeochemistry. Annu Rev Marine Sci 3: 147-171.

Wallman, K., Linke, P., Suess, E., Bohrmann, G., Sahling, H., Schlüter, M., *et al.* (1997) Quantifying fluid flow, solute mixing, and biogeochemical turnover at cold vents of the eastern Aleutian subduction zone. Geochim Cosmochim Acta 61: 5209-5219.

Wang, Q., Garrity, G.M., Tiedje, J.M., and Cole, J.R. (2007) Naïve Bayesian classifier for rapid assignment of rRNA sequences into the new bacterial taxonomy. Appl Environ Microbiol 73: 5261-5267.

Weisse, T., Scheffel, U., Stadler, P., and Foissner, W. (2013) Bromeliothrix metopoides, a boom and bust ciliate (Ciliophora, Colpodea) from tank bromeliads. Eur J Protistol 49:406-419.

Werne, J.P., Bass, M., and Damste, J.S.S. (2002) Molecular isotopic tracing of carbon flow and trophic relationships in a methane-supported benthic microbial community. Limnol Oceanogr 47: 1694-1701.

Wylezich, C., and Jurgens, K. (2011) Protist diversity in suboxic and sulfidic waters of the Black Sea. Environ Microbiol 13: 2939-2956.

Table and Figure Legends

Table 1. p-values and R values derived from ANOSIMS tests across a range of sample sets and environmental variables. The variables include the following comparisons: Substrate Type (carbonates vs. sediment), Habitat Type (active carbonates, low activity carbonates, clam bed sediments, microbial mat sediments, low activity sediments), Activity (active vs. low activity), Depth (sediment horizons in 3 cm intervals), Sulfide (sulfide concentration in 3 mM sulfide bins). TAG data refers to the iTAG-L4 data set. ANOSIMS results for the iTAG-OTU data set can be found in the supplemental material (Table S2). The values highlighted in bold and shaded grey are statistically significant ($P < 0.05$).

Table 2. Diversity indices for the microbial eukaryotic community in microbial mat, clam bed and low activity sediment cores from North (n = 7) and South (n =5) Hydrate Ridge across all three datasets of recovered 18S rRNA genes (T-RFLP, iTAG-OTU and iTAG-L4). Average richness (# of fragments, # of OTUs and number of classes, respectively for each dataset) and Shannon Diversity (H') with standard deviations are given for each sediment depth horizon across all of the data sets.

Table 3. Diversity indices for the microbial eukaryotic community in carbonates from North (n = 11) and South (n = 3) Hydrate Ridge from both iTAG data sets. Average richness (# of OTUs and number of classes, respectively for each dataset) and Shannon Diversity (H') with standard deviations are given for carbonates recovered from both active and low activity seep sites.

Figure 1. Map showing sampling areas (black squares) from North and South Hydrate Ridge (A) with contours every 50 m and labeled contours every 200 m. Zoomed in grids of the north (B)

and south (c) regions; locations were active sediments (microbial mat and clam cores; open triangles), low activity sediments (reference cores; black triangles), active carbonates (open circles) and low activity carbonates (closed circles) were collected. Units are in latitude and longitude. The regional map (A) was created with GMT (Generic Mapping Tools; http://gmt.soest.hawaii.edu/projects/gmt) using bathymetric data from NOAA's US Coastal Relief Model (Pacific Northwest), which is a 3 arc-second resolution digital elevation model (http://www.ngdc.noaa.gov/mgg/coastal/grddas08/grddas08.htm)

Figure 2. Average concentration of hydrogen sulfide (sold line) and sulfate (dashed line) with depth below microbial mats (n=5; left), clam beds (n=4; middle) and low activity sediments (n=3; right) from Hydrate Ridge.

Figure 3. Maximum-likelihood tree of 18S rRNA gene ciliate sequences (Super-group = SAR, Superphylum = Alveolata, Phylum = Ciliophora) from a representative microbial mat core and selected sequences from environmental surveys and cultures. Tree was constructed using RAxML 7.2.8 with 1000 rapid bootstrap inferences and GTRGAMMA rate approximation. Bootstrap probabilities are shown for nodes with support greater than 50%. Numbers in parentheses indicate the number of clones recovered from 0-3, 3-6 and 6-9 cm depth horizons respectively. Scale bar represents 0.3 substitutions per site.

Figure 4. (A) Percent contribution of 18S rRNA gene sequences (grouped by class) from clone libraries associated with the 0-3 cm , 3-6 cm, and 6-9 cm depth horizons in a microbial mat core from North HR. The corresponding sulfide ranges for each depth are given. (B) The relative abundance of ciliate classes in relationship to sulfide concentration from iTAG data across all

sediment samples (i.e., all habitats and all sediment depths). The relative abundance represents an average of all sequences within a ciliate class from all samples within each sulfide range.

Figure 5. Two-dimensional MDS plot visualizing the relationship of microbial eukaryotic composition across all habitats by class from the iTAG-L4 dataset. Each point represents sequences recovered from a 3-cm thick sediment interval or a carbonate rock. Open and filled symbols indicate activity level and the shape of the symbol indicates substrate type. Ellipses of standard deviation are shown for the data grouped by substrate type and the arrow indicates how the data are separated by activity. Note - active sediments include both microbial mat and clam bed sediments.

Figure 6. Two-dimensional MDS plot visualizing the relationship of microbial eukaryotic composition across all sediments in both the iTAG-L4 (A) and T-RFLP (B) datasets. Each point represents sequences recovered from a 3-cm thick sediment interval. Symbols are color coded by habitat (e.g., microbial mat, clam bed or low activity sediments). The size of the symbol represents the sulfide concentration (mM) measured in that sediment horizon. The outline color indicates whether those cores were collected from North or South Hydrate Ridge.

Figure 7. Relative abundance of a subset of microbial eukaryotes grouped by class from the iTAG-L4 dataset across all samples. See Fig. S4 for relative abundance of all taxa. The size of the symbol represents the relative abundance of that group within the entire microbial eukaryotic community and the color of the symbol indicates habitat type. In some cases class level has been designated as the prior rank followed by '_X' because there is not always agreement between experts at a given rank for some groups (see http://ssu-rrna.org/pr2 for more details on naming conventions).

Figure 8. Relationship between richness and sulfide concentration for all three data sets. Richness refers to the # of peaks (T-RFLP), number of microbial eukaryotic classes (TAG-L4), or number of OTUs (TAG-OTU) depending on the data set from which it was derived. Each point represents the average richness within a particular habitat and sulfide range. For example, all microbial mat cores within a particular sulfide range were averaged together. The error bars represent standard error. Closed symbols = HR North, open symbols = HR South.

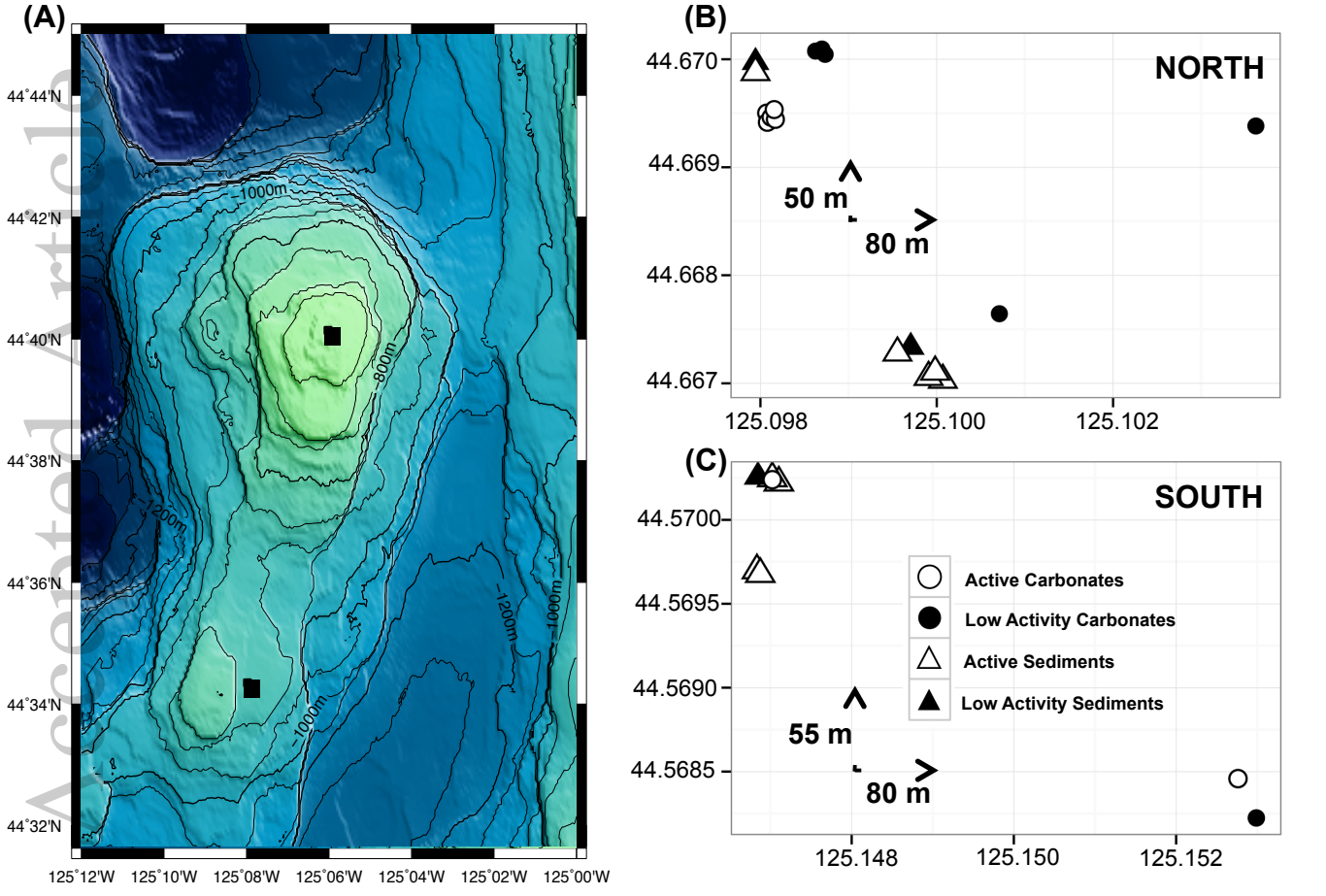

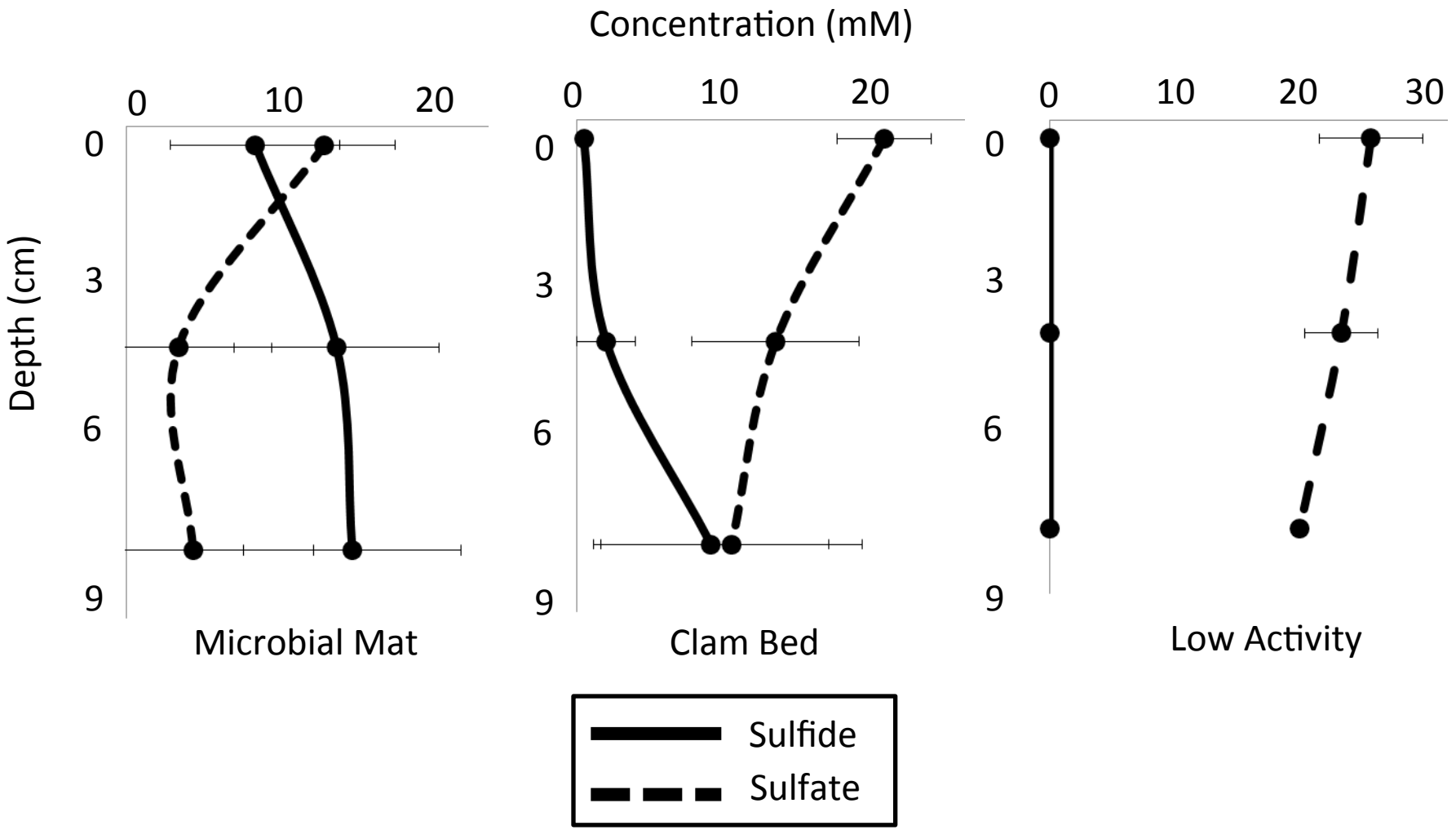
Concentration (mM)
0
10
20
0
10
20
0
10
20
30
Depth (cm)
0
3
6
9
0
3
6
9
0
3
6
9
Microbial Mat
Clam Bed
Low Activity
Sulfide
Sulfate


AF527757 Lechriopyla mystax
KT346301 HR_CIl_03_19, 1_0_0
KT346289 HR_CIl_03_18, 3_0_0
DQ103835 uncultured marine eukaryote anoxic Mariager Fjord
Z29442 Plagiopyla nasuta
AB505461 uncultured eukaryote microbial mats in deep-sea cold seep sediment
KT346294 HR_CIl_03_17, 3_0_0
KT346296 HR_CIl_03_16, 1_2_0
KT346312 HR_CIl_03_15, 3_0_0
AB505458 uncultured eukaryote microbial mats in deep-sea cold seep sediment
EF014286 Epalxella antiquorum Lake Alatsee
HM749918 uncultured marine eukaryote Black Sea redoxcline
GU819289 uncultured ciliate anoxic water column sample Cariaco Basin Caribbean Sea
AJ292526 Trimyema minutum thermophilum
FJ000101 uncultured eukaryote Bannock Basin interface environment Mediterranean Sea
KT346317 HR_CIl_36_14, 0_1_0
DQ310196 uncultured marine eukaryote super-sulfidic anoxic fjord water samples
KT346304 HR_CIl_03_20, 1_0_0
EF527104 uncultured marine eukaryote marine environment
GU819513 uncultured ciliate anoxic water column sample Cariaco Basin Caribbean Sea
KT346320 HR_CIl_36_22, 0_2_1
AY821925 uncultured ciliate total DNA isolated from fresh water filtrate
KT346316 HR_CIl_03_21, 1_0_1
AY821934 uncultured ciliate total DNA isolated from fresh water sediment
AF351579 Cryptocaryon irritans
AB505514 uncultured eukaryote microbial mats in deep-sea cold seep sediment
DQ103875 uncultured marine eukaryote anoxic Mariager Fjord
AB505464 uncultured eukaryote microbial mats in deep-sea cold seep sediment
KT346323 HR_CIl_69_12, 0_0_2
KT346303 HR_CIl_03_13, 1_0_0
DQ103796 uncultured marine eukaryote anoxic Mariager Fjord
KT346322 HR_CIl_69_11, 0_0_1
EF526814 uncultured marine eukaryote marine environment
HM749903 uncultured marine eukaryote Black Sea redoxcline
GU819262 uncultured ciliate anoxic water column Cariaco Basin Caribbean Sea
EF527129 uncultured marine eukaryote marine environment
GU819510 uncultured ciliate anoxic water column Cariaco Basin Caribbean Sea
Z29517 Cyclidium porcatum
KT346283 HR_CIl_03_10, 6_1_0
AB505463 uncultured eukaryote microbial mats in deep-sea cold seep sediment
KT346313 HR_CIl_03_9, 1_0_0
AB505511 uncultured eukaryote microbial mats in deep-sea cold seep sediment
FJ000241 uncultured eukaryote Discovery Basin interface environment Mediterranean Sea
EF527113 uncultured marine eukaryote marine environment
EF486864 Pleuronema sinica
KT346330 HR_CIl_69_8, 1_0_0
EF526877 uncultured marine eukaryote marine environment
EU032356 Cyclidium glaucoma
Phyllopharyngea
Nassophorea
Colpodida
KT346290 HR_CIl_03_42, 14_2_0
AB505469 uncultured eukaryote microbial mats in deep-sea cold seep sediment
KT346298 HR_CIl_03_43, 1_0_0
KT346306 HR_CIl_03_40, 1_0_0
KT346319 HR_CIl_36_41, 0_1_0
AB505517 uncultured eukaryote microbial mats in deep-sea cold seep sediment
KT346309 HR_CIl_03_35, 2_0_0
KT346299 HR_CIl_03_38, 51_4_0
KT346284 HR_CIl_03_36, 6_0_0
KT346318 HR_CIl_36_37, 0_2_1
KT346295 HR_CIl_03_34, 1_0_0
KT346315 HR_CIl_03_39, 1_0_0
GU819286 uncultured ciliate oxygenated water column Cariaco Basin Caribbean Sea
GU824939 uncultured eukaryote micro-oxic water column Cariaco Basin Caribbean Sea
AB505518 uncultured eukaryote microbial mats in deep-sea cold seep sediment
FJ814761 uncultured ciliate Carmel Canyon
AB505519 uncultured eukaryote microbial mats in deep-sea cold seep sediment
Oligotrichia
Choreotrichia
AB505474 uncultured eukaryote microbial mats in deep-sea cold seep sediment
KT346310 HR_CIl_03_6, 1_0_0
EF526963 uncultured marine eukaryote marine environment
AF530527 uncultured ciliate hydrothermal Mid Atlantic Ridge environments
FJ000242 uncultured eukaryote Discovery Basin interface environment Mediterranean Sea
AF370028 Oxytricha saltans
DQ103853 uncultured marine eukaryote anoxic Mariager Fjord
KT346311 HR_CIl_03_4, 12_0_0
KT346305 HR_CIl_03_5, 1_0_0
DQ057346 Trachelostyla pediculiformis
KT346302 HR_CIl_03_7, 1_0_0
AM412773 Oxytricha lanceolata
AB505523 uncultured eukaryote microbial mats in deep-sea cold seep sediment
KT346291 HR_CIl_03_3, 3_0_0
AB505522 uncultured eukaryote microbial mats in deep-sea cold seep sediment
KT346307 HR_CIl_03_1, 2_0_0
KT346308 HR_CIl_03_2, 1_0_0
EF123704 Aspidisca aculeata
DQ504338 uncultured ciliate Lost City
AB505477 uncultured eukaryote microbial mats in deep-sea cold seep sediment
EF100244 uncultured eukaryote oxygen-depleted intertidal marine sediment upper 2 cm
EF526985 uncultured marine eukaryote marine environment
KT346285 HR_CIl_03_33, 6_9_2
KT346292 HR_CIl_03_32, 6_0_0
KT346326 HR_CIl_69_31, 0_0_1
KT346288 HR_CIl_03_29, 1_0_0
GU819342 uncultured ciliate anoxic water column Cariaco Basin Caribbean Sea
GU819504 uncultured ciliate anoxic water column Cariaco Basin Caribbean Sea
KT346331 HR_CIl_69_28, 0_0_1
KT346327 HR_CIl_69_30, 0_0_1
AY179984 uncultured alveolate oxygen-depleted marine environment
KT346286 HR_CIl_03_26, 3_0_0
KT346314 HR_CIl_03_27, 1_0_0
KT346300 HR_CIl_03_25, 1_0_0
AY179982 uncultured alveolate oxygen-depleted marine environment
KT346287 HR_CIl_03_24, 1_0_0
AY007453 Metopus palaeformis
DQ310252 uncultured marine eukaryote super-sulfidic anoxic fjord water samples
KT346324 HR_CIl_69_23, 0_0_3
U97108 Caenomorpha uniserialis
AB505480 uncultured eukaryote microbial mats deep-sea cold seep sediment
DQ190465 Loxophyllum rostratum
AF530528 uncultured ciliate hydrothermal Mid Atlantic Ridge environments
DQ411858 Epispathidium papilliferum
AY179986 uncultured ciliate oxygen-depleted marine environment
KT346293 HR_CIl_03_44, 1_0_0
KT346328 HR_CIl_69_48, 0_0_1
KT346297 HR_CIl_03_49, 2_1_0
DQ845294 Mesodinium pulex
EF526944 uncultured marine eukaryote
AB505507 uncultured eukaryote microbial mats in deep-sea cold seep sediment
KT346325 HR_CIl_69_46, 0_0_1
KT346321 HR_CIl_03_45, 3_0_0
EF526714 uncultured marine eukaryote marine environment
KT346329 HR_CIl_69_47, 0_0_1
Heterotrichea
Karyorelictea
Dinoflagellata
Apicomplexa
Outgroup
0.3
Plagiopylea
Prostomatea
Oligohymenophorea
Novel Seep Clade
Spirotrichea
Cariacotrichea
Armophorea
Litostomatea

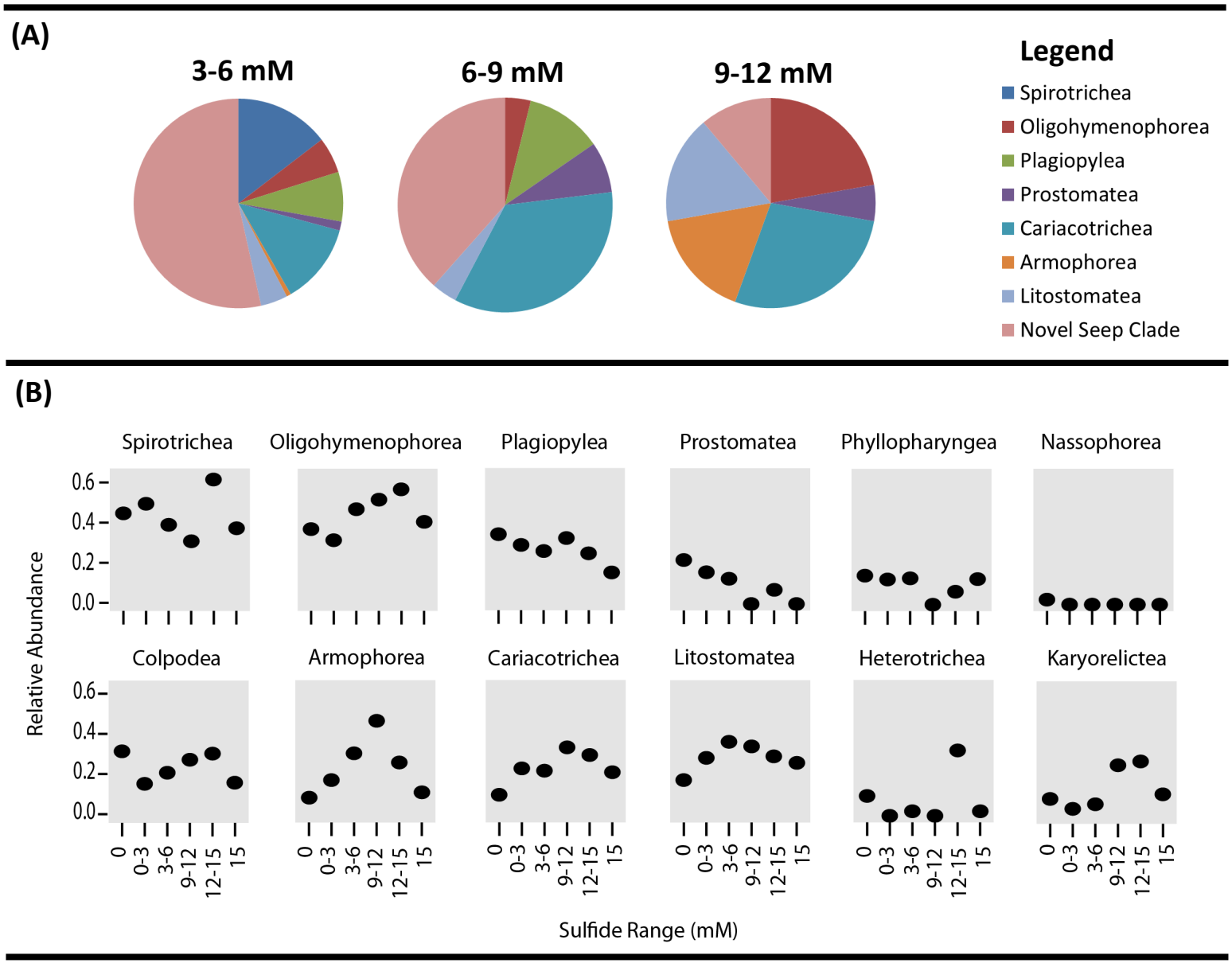
(A)
3-6 mM
6-9 mM
9-12 mM
Legend
Spirotrichea
Oligohymenophorea
Plagiopylea
Prostomatea
Cariacotrichea
Armophorea
Litostomatea
Novel Seep Clade
(B)
Spirotrichea
Oligohymenophorea
Plagiopylea
Prostomatea
Phyllopharyngea
Nassophorea
Colpodea
Armophorea
Cariacotrichea
Litostomatea
Heterotrichea
Karyorelictea
Relative Abundance
0.6
0.4
0.2
0.0
0
0-3
3-6
9-12
12-15
15
Sulfide Range (mM)

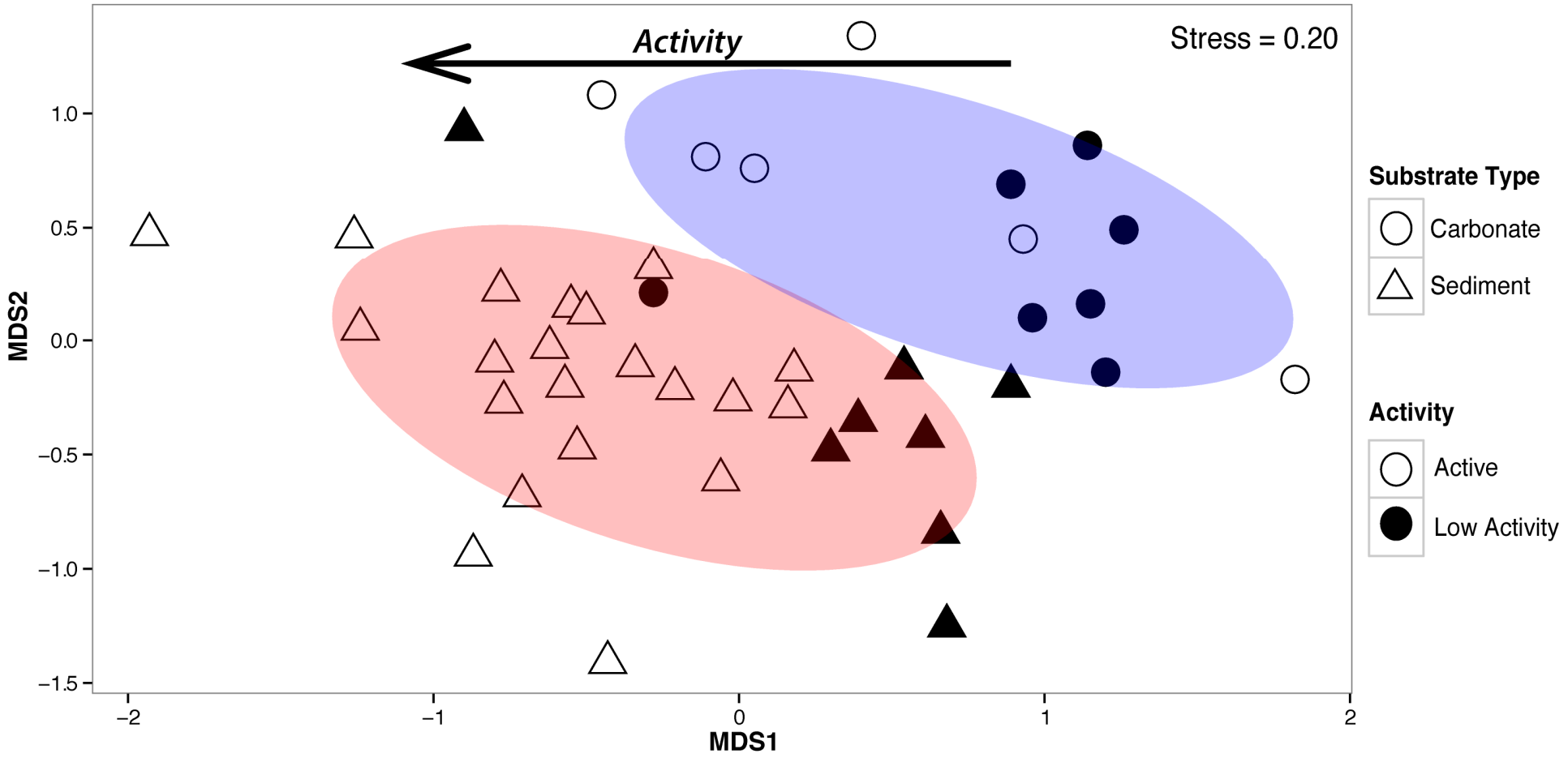
Activity
Stress = 0.20
MDS2
MDS1
1.0
0.5
0.0
−0.5
−1.0
−1.5
−2
−1
0
1
2
Substrate Type
Carbonate
Sediment
Activity
Active
Low Activity

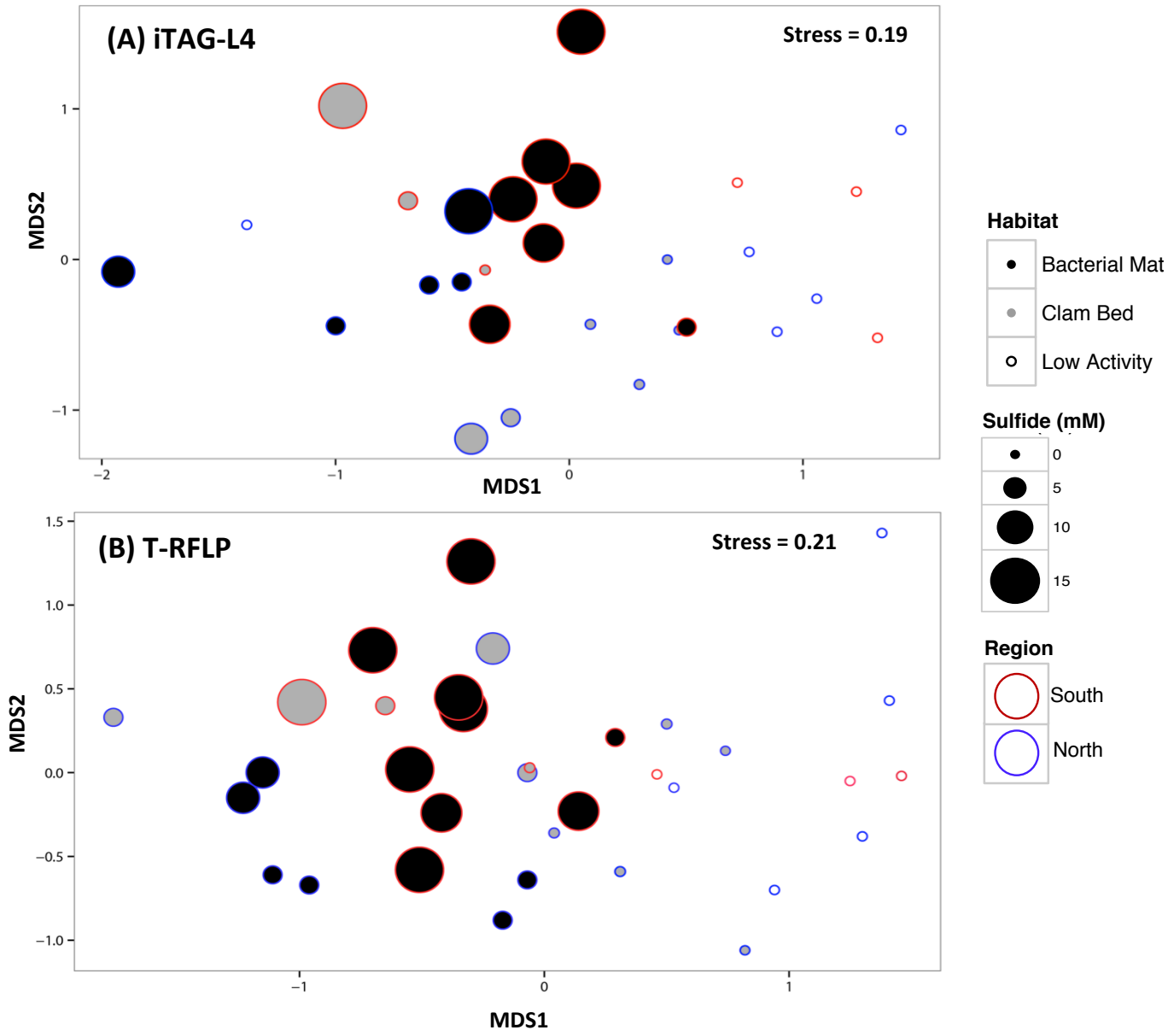
(A) iTAG-L4
Stress = 0.19
MDS2
MDS1
(B) T-RFLP
Stress = 0.21
MDS2
MDS1
Habitat
Bacterial Mat
Clam Bed
Low Activity
Sulfide (mM)
0
5
10
15
Region
South
North

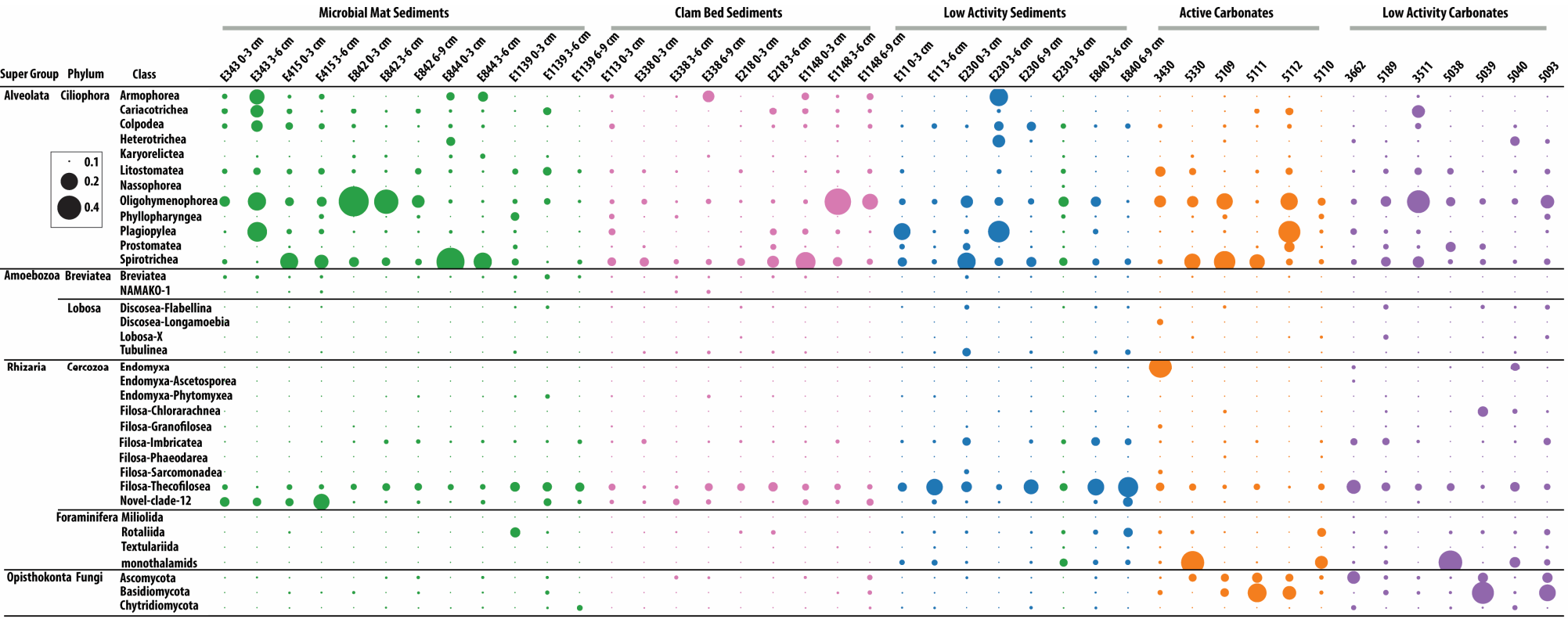
Microbial Mat Sediments
Clam Bed Sediments
Low Activity Sediments
Active Carbonates
Low Activity Carbonates
E343 0-3 cm
E343 3-6 cm
E415 0-3 cm
E415 3-6 cm
E842 0-3 cm
E842 3-6 cm
E842 6-9 cm
E844 0-3 cm
E844 3-6 cm
E1139 0-3 cm
E1139 3-6 cm
E1139 6-9 cm
E113 0-3 cm
E338 0-3 cm
E338 3-6 cm
E338 6-9 cm
E218 0-3 cm
E218 3-6 cm
E1148 0-3 cm
E1148 3-6 cm
E1148 6-9 cm
E110 3-6 cm
E113 3-6 cm
E230 0-3 cm
E230 3-6 cm
E230 6-9 cm
E230 3-6 cm
E840 3-6 cm
E840 6-9 cm
3430
5330
5109
5111
5112
5110
3662
5189
3511
5038
5039
5040
5093
Super Group
Phylum
Class
Alveolata
Ciliophora
Armophorea
Cariacotrichea
Colpodea
Heterotrichea
Karyorelictea
Litostomatea
Nassophorea
Oligohymenophorea
Phyllopharyngea
Plagiopylea
Prostomatea
Spirotrichea
0.1
0.2
0.4
Amoebozoa
Breviatea
Breviatea
NAMAKO-1
Lobosa
Discosea-Flabellina
Discosea-Longamoebia
Lobosa-X
Tubulinea
Rhizaria
Cercozoa
Endomyxa
Endomyxa-Ascetosporea
Endomyxa-Phytomyxea
Filosa-Chlorarachnea
Filosa-Granofilosea
Filosa-Imbricatea
Filosa-Phaeodarea
Filosa-Sarcomonadea
Filosa-Thecofilosea
Novel-clade-12
Foraminifera
Miliolida
Rotaliida
Textulariida
monothalamids
Opisthokonta
Fungi
Ascomycota
Basidiomycota
Chytridiomycota

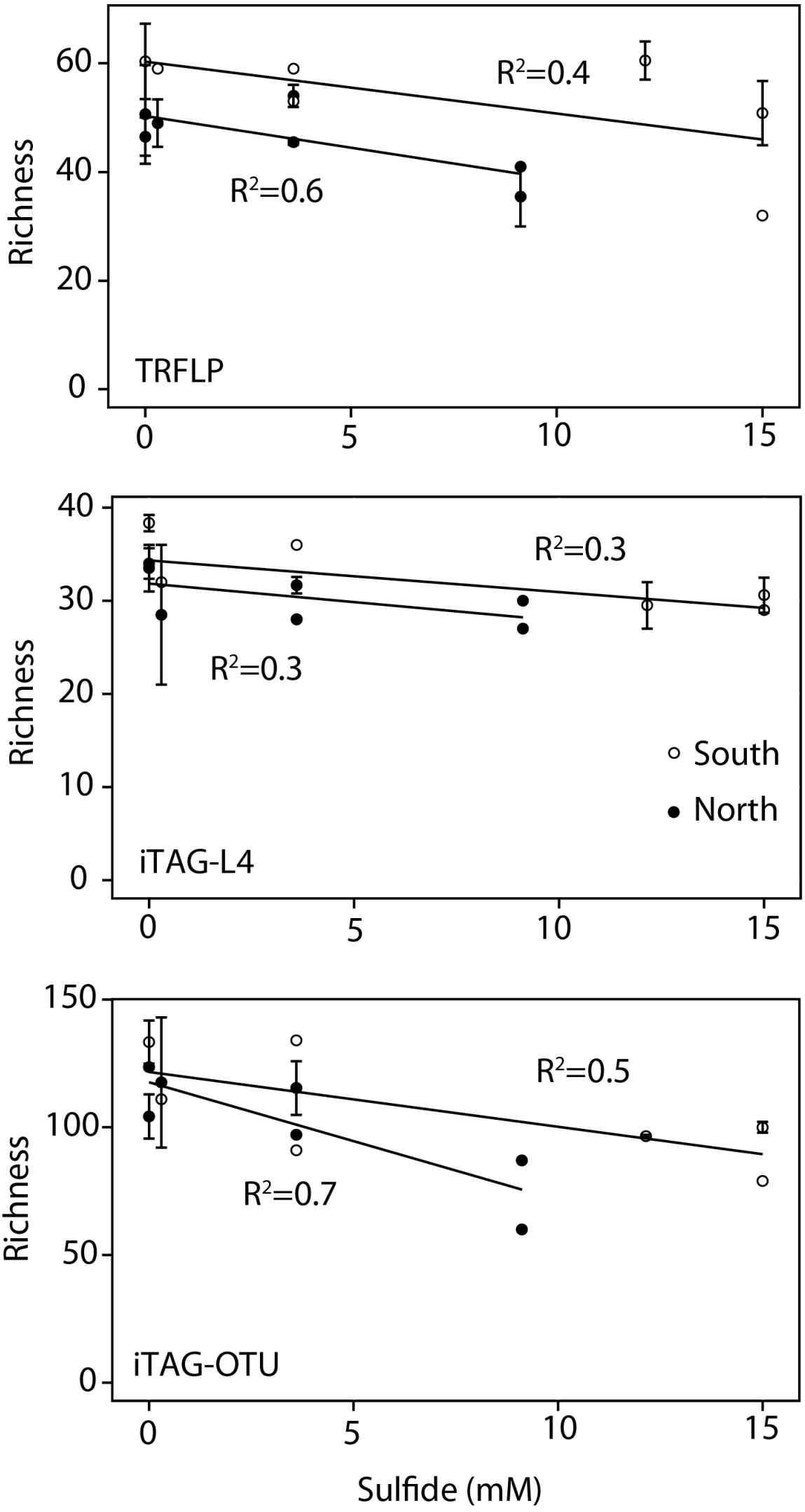
Richness
60
40
20
0
R²=0.4
R²=0.6
TRFLP
0
5
10
15
Richness
40
30
20
10
0
R²=0.3
R²=0.3
South
North
iTAG-L4
0
5
10
15
Richness
150
100
50
0
R²=0.5
R²=0.7
iTAG-OTU
0
5
10
15
Sulfide (mM)

Sample Set		Environmental Groupings											
		Region		Substrate Type		Habitat Type		Activity		Depth		Sulfide	
		TAG	TRFLP	TAG	TRFLP	TAG	TRFLP	TAG	TRFLP	TAG	TRFLP	TAG	TRFLP
All Habitats	Global R	0.07	--	**0.44**	--	**0.4**	--	**0.3**	--	--	--	--	--
	p-value	0.09	--	**0.001**	--	**0.001**	--	**0.001**	--	--	--	--	--
All Carbonates	Global R	0.3	--	--	--	--	--	**0.2**	--	--	--	--	--
	p-value	0.06	--	--	--	--	--	**0.04**	--	--	--	--	--
All Sediments	Global R	**0.2**	**0.1**	--	--	**0.2**	**0.3**	**0.5**	**0.5**	**0.2**	**0.1**	**0.4**	**0.4**
	p-value	**0.01**	**0.04**	--	--	**0.001**	**0.001**	**0.001**	**0.001**	**0.01**	**0.02**	**0.001**	**0.001**
Active Sediments	Global R	**0.2**	**0.2**	--	--	0.02	0.04	--	--	**0.3**	**0.3**	**0.3**	**0.3**
	p-value	**0.006**	**0.001**	--	--	0.4	0.3	--	--	**0.004**	**0.001**	**0.009**	**0.001**
Low Activity Sediments	Global R	-0.06	-0.1	--	--	--	--	--	--	-0.12	-0.05	--	--
	p-value	0.6	0.7	--	--	--	--	--	--	0.7	0.6	--	--
Clam Beds	Global R	**0.6**	0.08	--	--	--	--	--	--	0.2	0.1	0.3	0.3
	p-value	**0.01**	0.4	--	--	--	--	--	--	0.1	0.2	0.1	0.1
Microbial Mats	Global R	**0.3**	**0.5**	--	--	--	--	--	--	0.2	**0.3**	**0.5**	**0.5**
	p-value	**0.04**	**0.001**	--	--	--	--	--	--	0.1	**0.01**	**0.001**	**0.003**

			Microbial Mat		Clam Bed		Low Activity	
		Metric	North	South	North	South	North	South
TRFLP	0-3 cm	Richness	51.5 ± 3.5	60 ± 3.6	47 ± 5.2	59	50 ± 12.7	72
		H'(log_e)	3.9 ± 0.07	4.0 ± 0.05	3.8 ± 0.1	4	3.8 ± 0.3	4.2
	3-6 cm	Richness	50 ± 12.7	56 ± 4.3	44.6 ± 1.5	53	38.5 ± 23.2	48
		H'(log_e)	3.9 ± 0.3	3.9 ± 0.07	3.7 ± 0.03	3.9	3.5 ± 0.6	3.8
	6.9 cm	Richness	42 ± 17	45.6 ± 20.6	48 ± 10.6	32	76	61
		H'(log_e)	3.6 ± 0.4	3.7 ± 0.5	3.8 ± 0.2	3.4	4.3	4.1
TAG-L4	0-3 cm	Richness	31.5 ± 2.1	31.7 ± 4.5	29.3 ± 7.6	32	33 ± 1.4	38
		H'(log_e)	2.4 ± 0.04	2.06 ± 0.4	1.9 ± 0.4	2.4	2.4 ± 0.4	2.6
	3-6 cm	Richness	29.5 ± 3.5	31 ± 4.4	32 ± 5.7	28	33.5 ± 6.4	37
		H'(log_e)	2.4 ± 0.2	2.4 ± 0.2	2.1 ± 0.3	2.1	2.4 ± 0.06	2.7
	6-9 cm	Richness	--	30 ± 5.7	30	29	37	40
		H'(log_e)	--	2.2 ± 0.2	2.2	2.4	2.3	2.7
TAG-OTU	0-3 cm	Richness	108 ± 18.4	109 ± 21.7	119.6 ± 25.8	111	98.5 ± 7.8	150
		H'(log_e)	3.7 ± 0.3	3.1 ± 0.9	3.7 ± 0.4	3.7	3.6 ± 0.3	4.1
	3-6 cm	Richness	95 ± 49.5	99 ± 6.2	110 ± 18.4	91	98 ± 26.9	127
		H'(log_e)	3.4 ± 0.8	3.6 ± 0.5	3.7 ± 0.06	3.06	3.6 ± 0.5	4.2
	6.9 cm	Richness	--	101.5 ± 2.1	87	79	128	123
		H'(log_e)	--	3.5 ± 0.08	3.5	3.6	3.9	3.9

		Metric	North	South
iTAG-L4	Active	Richness	29.1 ± 2.4	30 ± 7.1
		H'(log_e)	2.4 ± 0.1	2.4 ± 0.1
	Low Activity	Richness	34.3 ± 5.8	40
		H'(log_e)	2.5 ± 0.3	2.5
iTAG-OTU	Active	Richness	93.3 ± 25.5	88 ± 7.1
		H'(log_e)	3.4 ± 0.4	3.4 ± 0.2
	Low Activity	Richness	113.6 ± 22.8	117
		H'(log_e)	3.7 ± 0.4	3.8